Cavity Opto-Mechanics

T.J. Kippenberg[1] **and K.J. Vahala**[2]

[1]*Max Planck Institut für Quantenoptik, Garching, Germany*
[2]*California Institute of Technology, Pasadena, USA*

[1]*tjk@mpq.mpg.de*,[2]*vahala@caltech.edu*

Abstract: The coupling of mechanical and optical degrees of freedom via radiation pressure has been a subject of early research in the context of gravitational wave detection. Recent experimental advances have allowed studying for the first time the modifications of mechanical dynamics provided by radiation pressure. This paper reviews the consequences of back-action of light confined in whispering-gallery dielectric micro-cavities, and presents a unified treatment of its two manifestations: notably the parametric instability (mechanical amplification and oscillation) and radiation pressure back-action cooling. Parametric instability offers a novel ”photonic clock” which is driven purely by the pressure of light. In contrast, radiation pressure cooling can surpass existing cryogenic technologies and offers cooling to phonon occupancies below unity and provides a route towards cavity Quantum Optomechanics

OCIS codes: (140.3320) Laser cooling, (140.4780) Lasers and laser optics : Optical resonators, (230.1150) Optical devices : All-optical devices, (140.3945) Microcavities

References and links

1. K. J. Vahala, “Optical microcavities,” Nature **424**(6950), 839–846 (2003).
2. H. G. Craighead, “Nanoelectromechanical systems,” Science **290**(5496), 1532–1535 (2000).
3. T. W. Hansch and A. L. Schawlow, “Cooling of Gases by Laser Radiation,” Optics Communications **13**(1), 68–69 (1975).
4. D. J. Wineland, R. E. Drullinger, and F. L. Walls, “Radiation-Pressure Cooling of Bound Resonant Absorbers,” Physical Review Letters **40**(25), 1639–1642 (1978).
5. S. Chu, L. Hollberg, J. E. Bjorkholm, A. Cable, and A. Ashkin, “3-Dimensional Viscous Confinement and Cooling of Atoms by Resonance Radiation Pressure,” Physical Review Letters **55**(1), 48–51 (1985).
6. S. Stenholm, “The Semiclassical Theory of Laser Cooling,” Reviews of Modern Physics **58**(3), 699–739 (1986).
7. C. M. Caves, “Quantum-Mechanical Noise in an Interferometer,” Physical Review D **23**(8), 1693–1708 (1981).
8. K. Jacobs, I. Tittonen, H. M. Wiseman, and S. Schiller, “Quantum noise in the position measurement of a cavity mirror undergoing Brownian motion,” Physical Review A **60**(1), 538–548 (1999).
9. I. Tittonen, G. Breitenbach, T. Kalkbrenner, T. Muller, R. Conradt, S. Schiller, E. Steinsland, N. Blanc, and N. F. de Rooij, “Interferometric measurements of the position of a macroscopic body: Towards observation of quantum limits,” Physical Review A **59**(2), 1038–1044 (1999).
10. V. B. Braginsky, *Measurement of Weak Forces in Physics Experiments* (University of Chicago Press, Chicago, 1977).
11. V. B. Braginsky and F. Khalili, *Quantum Measurement* (Cambridge University Press, 1992).
12. S. Mancini and P. Tombesi, “Quantum-Noise Reduction by Radiation Pressure,” Physical Review A **49**(5), 4055–4065 (1994).
13. S. Bose, K. Jacobs, and P. L. Knight, “Preparation of nonclassical states in cavities with a moving mirror,” Physical Review A **56**(5), 4175–4186 (1997).
14. L. Tian and P. Zoller, “Coupled ion-nanomechanical systems,” Physical Review Letters **93**(26), 266,403 (2004).
15. M. D. LaHaye, O. Buu, B. Camarota, and K. C. Schwab, “Approaching the quantum limit of a nanomechanical resonator,” Science **304**(5667), 74–77 (2004).

#88348 - $15.00 USD Received 8 Oct 2007; revised 7 Dec 2007; accepted 7 Dec 2007; published 10 Dec 2007

16. A. Naik, O. Buu, M. D. LaHaye, A. D. Armour, A. A. Clerk, M. P. Blencowe, and K. C. Schwab, "Cooling a nanomechanical resonator with quantum back-action," Nature **443**(7108), 193–196 (2006).
17. I. Wilson-Rae, P. Zoller, and A. Imamoglu, "Laser cooling of a nanomechanical resonator mode to its quantum ground state," Physical Review Letters **92**(7), 075,507 (2004).
18. K. Brown, J. Britton, R. Epstein, J. Chiaverini, D. Leibfried, and D. Wineland, "Passive Cooling of a Micromechanical Oscillator with a Resonant Electric Circuit," Physical Review Letters **99**, 137,205 (2007).
19. A. Dorsel, J. D. McCullen, P. Meystre, E. Vignes, and H. Walther, "Optical Bistability and Mirror Confinement Induced by Radiation Pressure," Physical Review Letters **51**(17), 1550–1553 (1983).
20. B. S. Sheard, M. B. Gray, C. M. Mow-Lowry, D. E. McClelland, and S. E. Whitcomb, "Observation and characterization of an optical spring," Physical Review A **69**(5) (2004).
21. V. B. Braginsky, S. E. Strigin, and S. P. Vyatchanin, "Parametric oscillatory instability in Fabry-Perot interferometer," Physics Letters A **287**(5-6), 331–338 (2001).
22. T. J. Kippenberg, H. Rokhsari, T. Carmon, A. Scherer, and K. J. Vahala, "Analysis of Radiation-Pressure Induced Mechanical Oscillation of an Optical Microcavity," Physical Review Letters **95**, 033,901 (2005).
23. H. Rokhsari, T. J. Kippenberg, T. Carmon, and K. J. Vahala, "Radiation-pressure-driven micro-mechanical oscillator," Optics Express **13**(14), 5293–5301 (2005).
24. T. Carmon, H. Rokhsari, L. Yang, T. J. Kippenberg, and K. J. Vahala, "Temporal behavior of radiation-pressure-induced vibrations of an optical microcavity phonon mode," Physical Review Letters **94**(22) (2005).
25. V. B. Braginsky and S. P. Vyatchanin, "Low quantum noise tranquilizer for Fabry-Perot interferometer," Physics Letters A **293**(5-6), 228–234 (2002).
26. O. Arcizet, P. F. Cohadon, T. Briant, M. Pinard, and A. Heidmann, "Radiation-pressure cooling and optomechanical instability of a micromirror," Nature **444**(7115), 71–74 (2006).
27. S. Gigan, H. R. Bohm, M. Paternostro, F. Blaser, G. Langer, J. B. Hertzberg, K. C. Schwab, D. Bauerle, M. Aspelmeyer, and A. Zeilinger, "Self-cooling of a micromirror by radiation pressure," Nature **444**(7115), 67–70 (2006).
28. A. Schliesser, P. Del'Haye, N. Nooshi, K. J. Vahala, and T. J. Kippenberg, "Radiation pressure cooling of a micromechanical oscillator using dynamical backaction," Physical Review Letters **97**(24), 243,905 (2006).
29. T. Corbitt, Y. B. Chen, E. Innerhofer, H. Muller-Ebhardt, D. Ottaway, H. Rehbein, D. Sigg, S. Whitcomb, C. Wipf, and N. Mavalvala, "An all-optical trap for a gram-scale mirror," Physical Review Letters **98**, 150,802 (2007).
30. J. D. Thompson, B. M. Zwickl, A. M. Yarich, F. Marquardt, S. M. Girvin, and J. Harris, "Strong dispersive coupling of a high finesse cavity to a micromechanical membrane," arXiv:0707.1724 (2007).
31. S. Mancini, D. Vitali, and P. Tombesi, "Optomechanical cooling of a macroscopic oscillator by homodyne feedback," Physical Review Letters **80**(4), 688–691 (1998).
32. P. F. Cohadon, A. Heidmann, and M. Pinard, "Cooling of a mirror by radiation pressure," Physical Review Letters **83**(16), 3174–3177 (1999).
33. S. Vandermeer, "Stochastic Cooling and the Accumulation of Antiprotons," Reviews of Modern Physics **57**(3), 689–697 (1985).
34. D. Kleckner and D. Bouwmeester, "Sub-kelvin optical cooling of a micromechanical resonator," Nature **444**(7115), 75–78 (2006).
35. M. Poggio, C. L. Degen, H. J. Mamin, and D. Rugar, "Feedback cooling of a cantilever's fundamental mode below 5 mK," Physical Review Letters **99**(1) (2007).
36. O. Arcizet, P. F. Cohadon, T. Briant, M. Pinard, A. Heidmann, J. M. Mackowski, C. Michel, L. Pinard, O. Francais, and L. Rousseau, "High-sensitivity optical monitoring of a micromechanical resonator with a quantum-limited optomechanical sensor," Physical Review Letters **97**(13), 133,601 (2006).
37. V. Giovannetti, S. Mancini, and P. Tombesi, "Radiation pressure induced Einstein-Podolsky-Rosen paradox," Europhysics Letters **54**(5), 559–565 (2001).
38. S. Mancini, V. Giovannetti, D. Vitali, and P. Tombesi, "Entangling macroscopic oscillators exploiting radiation pressure," Physical Review Letters **88**(12), 120,401 (2002).
39. J. M. Courty, A. Heidmann, and M. Pinard, "Quantum locking of mirrors in interferometers," Physical Review Letters **90**(8) (2003).
40. O. Arcizet, T. Briant, A. Heidmann, and M. Pinard, "Beating quantum limits in an optomechanical sensor by cavity detuning," Physical Review A **73**(3) (2006).
41. W. Marshall, C. Simon, R. Penrose, and D. Bouwmeester, "Towards quantum superpositions of a mirror," Physical Review Letters **91**(13) (2003).
42. M. Hossein-Zadeh and K. J. Vahala, "Photonic RF Down-Converter Based on Optomechanical Oscillation," (to be published).
43. M. L. Povinelli, J. M. Johnson, M. Loncar, M. Ibanescu, E. J. Smythe, F. Capasso, and J. D. Joannopoulos, "High-Q enhancement of attractive and repulsive optical forces between coupled whispering-gallery-mode resonators," Optics Express **13**(20), 8286–8295 (2005).
44. M. Eichenfeld, C. Michael, R. Perahia, and O. Painter, "Actuation of Micro-Optomechanical Systems Via Cavity-Enhanced Optical Dipole Forces," Nature Photonics **1**(7), 416 (2007).
45. K. C. Schwab and M. L. Roukes, "Putting mechanics into quantum mechanics," Physics Today **58**(7), 36–42

#88348 - $15.00 USD Received 8 Oct 2007; revised 7 Dec 2007; accepted 7 Dec 2007; published 10 Dec 2007

(2005).
46. Y. Akahane, T. Asano, B. S. Song, and S. Noda, "High-Q photonic nanocavity in a two-dimensional photonic crystal," Nature **425**(6961), 944–947 (2003).
47. A. Schliesser, R. Riviere, G. Anetsberger, O. Arcizet, and I. J. Kippenberg, "Demonstration of Resolved Sideband Cooling of a Mechanical Oscillator," http://arxiv.org/abs/0709.4036 (2007).
48. F. Marquardt, J. P. Chen, A. A. Clerk, and S. M. Girvin, "Quantum Theory of Cavity-Assisted Sideband Cooling of Mechanical Motion," Physical Review Letters **99**, 093,902 (2007).
49. I. Wilson-Rae, N. Nooshi, W. Zwerger, and T. J. Kippenberg, "Theory of Ground State Cooling of a Mechanical Oscillator Using Dynamical Backaction," Physical Review Letters **99**, 093,902 (2007).
50. C. K. Law, "Interaction between a Moving Mirror and Radiation Pressure - a Hamiltonian-Formulation," Physical Review A **51**(3), 2537–2541 (1995).
51. H. A. Haus, *Electromagnetic fields and energy* (Prentice Hall, Englewood Cliff, 1989).
52. M. Pinard, Y. Hadjar, and A. Heidmann, "Effective mass in quantum effects of radiation pressure," European Physical Journal D **7**(1), 107–116 (1999).
53. F. Marquardt, J. Harris, and S. Girvin, "Dynamical Multistability Induced by Radiation Pressure in High-Finesse Micromechanical Optical Cavities," Physical Review Letters **96**(103901-1) (2006).
54. M. Hossein-Zadeh and K. J. Vahala, "Observation of optical spring effect in a microtoroidal optomechanical resonator," Optics Letters **32**(12), 1611–1613 (2007).
55. K. Karrai, "Photonics - A cooling light breeze," Nature **444**(7115), 41–42 (2006).
56. V. Vuletic and S. Chu, "Laser cooling of atoms, ions, or molecules by coherent scattering," Physical Review Letters **84**(17), 3787–3790 (2000).
57. P. Maunz, T. Puppe, I. Schuster, N. Syassen, P. W. H. Pinkse, and G. Rempe, "Cavity cooling of a single atom," Nature **428**(6978), 50–52 (2004).
58. V. B. Braginsky, M. L. Gorodetsky, and V. S. Ilchenko, "Quality-Factor and Nonlinear Properties of Optical Whispering- Gallery Modes," Physics Letters A **137**(7-8), 393–397 (1989).
59. T. J. Kippenberg, S. M. Spillane, D. K. Armani, and K. J. Vahala, "Fabrication and coupling to planar high-Q silica disk microcavities," Applied Physics Letters **83**(4), 797–799 (2003).
60. D. K. Armani, T. J. Kippenberg, S. M. Spillane, and K. J. Vahala, "Ultra-high-Q toroid microcavity on a chip," Nature **421**(6926), 925–928 (2003).
61. R. Ma, A. Schliesser, P. Del'Haye, A. Dabirian, G. Anetsberger, and T. J. Kippenberg, "Radiation-pressure-driven vibrational modes in ultrahigh-Q silica microspheres," Optics Letters **32**(15), 2200–2202 (2007).
62. T. Carmon, M. C. Cross, and K. J. Vahala, "Chaotic quivering of micron-scaled on-chip resonators excited by centrifugal optical pressure," Physical Review Letters **98**(16) (2007). 0031-9007.
63. T. Carmon and K. J. Vahala, "Modal spectroscopy of optoexcited vibrations of a micron-scale on-chip resonator at greater than 1 GHz frequency," Physical Review Letters **98**(12) (2007).
64. S. M. Spillane, T. J. Kippenberg, O. J. Painter, and K. J. Vahala, "Ideality in a fiber-taper-coupled microresonator system for application to cavity quantum electrodynamics," Physical Review Letters **91**(4), art. no.–043,902 (2003).
65. S. M. Spillane, T. J. Kippenberg, and K. J. Vahala, "Ultralow-threshold Raman laser using a spherical dielectric microcavity," Nature **415**(6872), 621–623 (2002).
66. T. J. Kippenberg, S. M. Spillane, and K. J. Vahala, "Kerr-nonlinearity optical parametric oscillation in an ultrahigh-Q toroid microcavity," Physical Review Letters **93**(8) (2004).
67. M. Hossein-Zadeh, H. Rokhsari, A. Hajimiri, and K. J. Vahala, "Characterization of a radiation-pressure-driven micromechanical oscillator," Physical Review A **74**(2) (2006).
68. C. H. Metzger and K. Karrai, "Cavity cooling of a microlever," Nature **432**(7020), 1002–1005 (2004).
69. T. Carmon, L. Yang, and K. J. Vahala, "Dynamical thermal behavior and thermal self-stability of microcavities," Optics Express **12**(20), 4742–4750 (2004).
70. G. Bjorklund, M. Levenson, W. Lenth, and C. Ortiz, "Frequency modulation (FM) spectroscopy," Applied Physics B Lasers and Optics **32**(3), 145–152 (1983).
71. M. Zalalutdinov, A. Zehnder, A. Olkhovets, S. Turner, L. Sekaric, B. Ilic, D. Czaplewski, J. M. Parpia, and H. G. Craighead, "Autoparametric optical drive for micromechanical oscillators," Applied Physics Letters **79**(5), 695–697 (2001).
72. F. Treussart, V. S. Ilchenko, J. F. Roch, J. Hare, V. Lefevre-Seguin, J. M. Raimond, and S. Haroche, "Evidence for intrinsic Kerr bistability of high-Q microsphere resonators in superfluid helium," European Physical Journal D **1**(3), 235–238 (1998).
73. H. Rokhsari and K. J. Vahala, "Observation of Kerr nonlinearity in microcavities at room temperature," Optics Letters **30**(4), 427–429 (2005).
74. F. Diedrich, J. C. Bergquist, W. M. Itano, and D. J. Wineland, "Laser Cooling to the Zero-Point Energy of Motion," Physical Review Letters **62**(4), 403–406 (1989).
75. D. M. Meekhof, C. Monroe, B. E. King, W. M. Itano, and D. J. Wineland, "Generation of nonclassical motional states of a trapped atom," Physical Review Letters **76**(11), 1796–1799 (1996).
76. C. Monroe, D. M. Meekhof, B. E. King, and D. J. Wineland, "A "Schrodinger cat" superposition state of an

#88348 - $15.00 USD Received 8 Oct 2007; revised 7 Dec 2007; accepted 7 Dec 2007; published 10 Dec 2007

atom," Science **272**(5265), 1131–1136 (1996).
77. D. Leibfried, R. Blatt, C. Monroe, and D. Wineland, "Quantum dynamics of single trapped ions," Reviews of Modern Physics **75**(1), 281–324 (2003).
78. D. J. Wineland and W. M. Itano, "Laser Cooling of Atoms," Physical Review A **20**(4), 1521–1540 (1979).
79. H. J. Kimble, "Strong interactions of single atoms and photons in cavity QED," Physica Scripta **T76**, 127–137 (1998).
80. V. B. Braginsky, S. E. Strigin, and S. P. Vyatchanin, "Analysis of parametric oscillatory instability in power recycled LIGO interferometer," Physics Letters A **305**(3-4), 111–124 (2002).
81. T. Corbitt, D. Ottaway, E. Innerhofer, J. Pelc, and N. Mavalvala, "Measurement of radiation-pressure-induced optomechanical dynamics in a suspended Fabry-Perot cavity," Physical Review A **74**(2) (2006).

1. Introduction

Recent years have witnessed a series of developments at the intersection of two, previously distinct subjects. Optical (micro-)cavities [1] and micro (nano) mechanical resonators [2], each a subject in their own right with a rich scientific and technological history, have, in a sense, become entangled experimentally by the underlying mechanism of optical, radiation pressure forces. These forces and their related physics have been of major interest in the field of atomic physics [3–6] for over 5 decades and the emerging opto-mechanical context has many parallels with this field.

The opto-mechanical coupling between a moving mirror and the radiation pressure of light has first appeared in the context of interferometric gravitational wave experiments. Owing to the discrete nature of photons, the quantum fluctuations of the radiation pressure forces give rise to the so called *standard quantum limit* [7–9]. In addition to this "*quantum back-action*" effect, the pioneering work of V. Braginsky [10] predicted that the radiation pressure of light, confined within an interferometer (or resonator), gives rise to the effect of dynamic back-action, which is a classical effect, that is caused by the finite cavity decay time. The resulting phenomena, which are the parametric instability (and associated mechanical amplification and oscillation) and opto-mechanical back-action cooling, represent *two sides of the same underlying "dynamic back-action" mechanism*. Later, theoretical work has proposed to use the radiation-pressure coupling for quantum non-demolition measurements of the light field [11], and as a means to create non-classical states of the light field [12] and the mechanical system [13]. It is noted that the effect of dynamic back-action is of rather general relevance and can occur outside of the opto-mechanical context. Indeed, related phenomena have been predicted to occur in systems where a mechanical oscillator is parametrically coupled to an electromagnetic resonant system, which can be either an electronic device, e.g. a Cooper-pair box [14], superconducting single electron transistor [15, 16], LC circuit [10], an optical resonance of a quantum dot [17] and have been observed experimentally in some of these schemes [10, 16, 18].

The experimental manifestations of optomechanical coupling by radiation pressure have been observable for some time. For instance, radiation pressure forces were observed in the pioneering work of H. Walther at the MPQ, manifesting themselves in radiation pressure (pondermotive) bistability [19], while even earlier work in the microwave domain had been carried out by Braginsky [10]. Moreover the modification of mechanical oscillator stiffness caused by radiation pressure, the "*optical spring*", have also recently been observed [20]. However, in contrast to these *static* manifestations of radiation pressure, the *dynamic* manifestations of radiation pressure forces on micro- and nano-mechanical objects have only recently become an experimental reality. Curiously, while the theory of dynamic back action was motivated by consideration of precision measurement in the context of gravitational wave detection using large interferometers [21], the first observation of this mechanism was reported in 2005 at a vastly different size scale in microtoroid cavities [22–24]. These observations were focused on the radiation pressure induced parametric instability [21]. Subsequently, the reverse

#88348 - $15.00 USD Received 8 Oct 2007; revised 7 Dec 2007; accepted 7 Dec 2007; published 10 Dec 2007

mechanism [25] (back-action cooling) has been exploited to cool cantilevers [26, 27], microtoroids [28] and macroscopic mirror modes [29] as well as mechanical nano-membranes [30]. We note that this technique is different than the earlier demonstrated radiation-pressure feedback cooling [31, 32], which uses electronic feedback analogous to "Stochastic Cooling" [33] of ions in storage rings and which can also provide very efficient cooling as demonstrated in recent experiments [34–36]. Indeed, research in this subject has experienced a remarkable acceleration over the past three years as researchers in diverse fields such as optical microcavities [1], micro and nano-mechanical resonators [2] and quantum optics pursue a common set of scientific goals set forward by a decade-old theoretical framework. Subjects ranging from entanglement [37, 38]; generation of squeezed states of light [12]; measurements at or beyond the standard quantum limit [11, 39, 40]; and even to tests of quantum theory itself are in play here [41]. On the practical side, there are opportunities to harness these forces for new metrology tools [36] and even for new functions on a semiconductor chip (e.g., oscillators [22, 23], optical mixers [42], and tuneable optical filters and switches [43, 44]. It seems clear that a new field of *cavity optomechanics* has emerged, and will soon evolve into *cavity quantum optomechanics* (cavity QOM) whose goal is the observation and exploration of quantum phenomena of mechanical systems [45] as well as quantum phenomena involving both photons and mechanical systems.

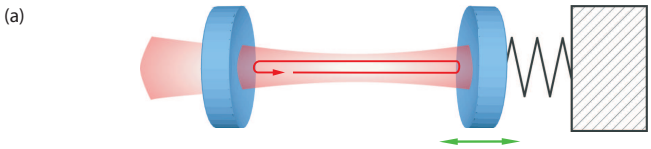

(b)

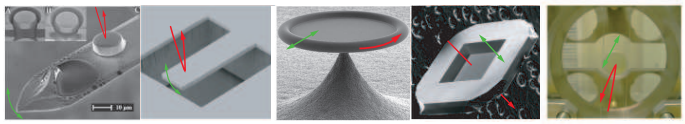

$\mathcal{F}$	200	30,000	22,000	15,000	4,000
$\Omega_m/2\pi$	12.5 kHz	814 kHz	57.8 MHz	134 kHz	12.7 Hz
Q_m	18,400	10,000	2,900	$1.1{\cdot}10^6$	19,950
m_{eff}	24 ng	190 µg	15 ng	40 ng	~1 g
Ref.	[34]	[26,27]	[22,28]	[30]	[29]

Fig. 1. (a)A cavity optomechanical system consisting of a Fabry Perot cavity with a harmonically bound end mirror. (b): Different physical realizations of cavity optomechanical experiments employing cantilevers [34], micro-mirrors [26, 27], micro-cavities [22, 28], nano-membranes [30] and macroscopic mirror modes [29]. Red and green arrows represent the optical trajectory and mechanical motion.

The realization of dynamical, opto-mechanical coupling in which radiation forces mediate the interaction, is a natural outcome of underlying improvements in the technologies of optical (micro) cavities and mechanical micro (nano-) resonators. Reduction of loss (increasing optical and mechanical Q) and reductions in form factor (modal volume) have enabled a regime of operation in which optical forces are dominant [22–24, 26–30]. This coupling also requires coexistence of high-Q optical and high-Q mechanical modes. Such coexistence has been achieved in the geometries illustrated in Figure 1. It also seems likely that other optical microcavity geometries such as photonic crystals [46] can exhibit the dynamic back-action effect provided that structures are modified to support high-Q mechanical modes.

To understand how the coupling of optical and mechanical degrees of freedom occurs in

#88348 - $15.00 USD Received 8 Oct 2007; revised 7 Dec 2007; accepted 7 Dec 2007; published 10 Dec 2007

any of the depicted geometries, one need only consider the schematic in the upper panel of Figure 1. Here, a Fabry-Perot optical cavity is assumed to feature a mirror that also functions as a mass-on-a-spring (i.e. is harmonically suspended). Such a configuration can indeed be encountered in gravitational wave laser interferometers (such as LIGO) and is also, in fact, a direct representation of the "cantilever mirror" embodiment in the lower panel within Figure 1. In addition, it is functionally equivalent to the case of a microtoroid embodiment (also shown in the lower panel), where the toroid itself provides both the optical modes as well as mechanical breathing modes (see discussion below). Returning to the upper panel, incident optical power that is resonant with a cavity mode creates a large circulating power within the cavity. This circulating power exerts a force upon the "mass-spring" mirror, thereby causing it to move. Reciprocally, the mirror motion results in a new optical round trip condition, which modifies the detuning of the cavity resonance with respect to the incident field. This will cause the system to simply establish a new, static equilibrium condition. The nonlinear nature of the coupling in such a case can manifest itself as a hysteretic behavior and was observed over two decades ago in the work by Walther et. al [19]. However, if the mechanical and optical Q's are sufficiently high (as is further detailed in what follows) a new set of dynamical phenomena can emerge, related to mechanical amplification and cooling.

In this paper, we will give the first unified treatment of this subject. Although microtoroid optical microcavities will be used as an illustrative platform, the treatment and phenomena are universal and pertain to any cavity opto-mechanical systems supporting high Q optical and mechanical modes. In what follows we begin with a theoretical framework through which dynamic back-action can be understood. The observation of micromechanical oscillation will then be considered by reviewing both old and new experimental results that illustrate the basic phenomena [22–24]. Although this mechanism has been referred to as the parametric instability, we show that it is more properly defined in the context of mechanical amplification and regenerative oscillation. For this reason, we introduce and define a mechanical gain, its spectrum, and, correspondingly, a threshold for oscillation. Mechanical cooling is introduced as the reverse mechanism to amplification. We will then review the experimental observation of cooling by dynamic back-action [28, 47] and also the quantum limits of cooling in microtoroids using back action [48, 49].

Finally, we will attempt to discuss some of the possible future directions for this new field of research.

2. Theoretical Framework of Dynamic Back-action

2.1. Coupled Mode Equations

Dynamic back-action is a modification of mechanical dynamics caused by non-adiabatic response of the optical field to changes in the cavity size. It can be understood through the coupled equations of motion for optical and mechanical modes, which can be derived from a single Hamiltonian [50].

$$\frac{da}{dt} = i\Delta(x)a - \left(\frac{1}{2\tau_0} + \frac{1}{2\tau_{ex}}\right)a + i\sqrt{\frac{1}{\tau_{ex}}}s \tag{1}$$

$$\frac{d^2x}{dt^2} + \frac{\Omega_m}{2Q_m}\frac{dx}{dt} + \Omega_m^2 x = \frac{F_{RP}(t)}{m_{eff}} + \frac{F_L(t)}{m_{eff}} = \frac{\zeta}{cm_{eff}}\frac{|a|^2}{T_{rt}} + \frac{F_L(t)}{m_{eff}} \tag{2}$$

Aside from the $x-$dependence, the first equation governs the dynamics of the optical field according to the formalism of H. Haus [51], i.e. $|a|^2$ is the stored cavity energy, whereas $|s|^2$ denotes the launched input power upon the cavity system. Moreover the optical field decays with a rate $\frac{1}{2\tau} = \frac{1}{2\tau_0} + \frac{1}{2\tau_{ex}}$and $\Delta(x) = \omega - \omega_0(x)$ accounts for the detuning of the pump laser

#88348 - $15.00 USD Received 8 Oct 2007; revised 7 Dec 2007; accepted 7 Dec 2007; published 10 Dec 2007

frequency ω with respect to the cavity resonance $\omega_0(x)$ (which, as shown below, depends on the mechanical coordinate, x). The power coupling rate into outgoing modes is described by the rate $1/\tau_{ex}$, whereas the intrinsic cavity loss rate is given by $1/\tau_0$. In the subsequent discussion, the photon decay rate is also used $\kappa \equiv 1/\tau$.

The second equation describes the mechanical coordinate (x) accounting for the movable cavity boundary (i.e. mirror), which is assumed to be harmonically bound and undergoing harmonic oscillation at frequency Ω_m with a power dissipation rate $\Gamma_m = \frac{\Omega_m}{Q_m}$. Moreover, m_{eff} is the effective mass of the mirror mode and will be discussed in a later section. This mass describes in large part the strength of the coupling between optical and mechanical modes. For an excellent treatment of its determination and derivation the reader is referred to reference [52]. The radiation pressure forcing function is given by $F_{RP}(t) = \frac{\zeta}{c}\frac{|a|^2}{T_{rt}}$, where the dimensionless parameter ζ takes on the value $2\pi n$ for a whispering-gallery-mode micro-cavity (consisting of a dielectric material with refractive index n), and $\zeta = 2$ for a Fabry Perot cavity; and where T_{rt} is the cavity round trip time (note that the intracavity circulating power is given by $\frac{|a|^2}{T_{rt}}$). Moreover the term $F_L(t)$ denotes the random Langevin force, and obeys $\langle F_L(t)F_L(t')\rangle = \Gamma_m k_B T_R m_{eff}\delta(t-t')$, where k_B is the Boltzmann constant and T_R is the temperature of the reservoir. The Langevin force ensures that the fluctuation dissipation theorem is satisfied, such that the total steady state energy without laser pumping is given by $E_m = \int \Omega^2 m_{eff}\left|\chi(\Omega)F_L(\Omega)\right|^2 d\Omega = k_B T_R$, where the mechanical susceptibility $\chi(\Omega) = m_{eff}^{-1}/(i\Omega\Gamma_m + \Omega_m^2 - \Omega^2)$ has been introduced. Of special interest in the first equation is the optical detuning $\Delta(x)$ which provides coupling to the second equation through the relation:

$$\Delta(x) = \Delta + \frac{\omega_0}{R}x \tag{3}$$

This relation assumes that, under circumstances in which the mass-spring is at rest $(x = 0)$, the optical pump is detuned by Δ relative to the optical mode resonance. Two cases of interest, both illustrated in Figure 2, will emerge: blue detuned ($\Delta > 0$) and red-detuned ($\Delta < 0$) operation of the pump-wave relative to the cavity resonance. It is important to note that quadratic coupling can also be realized, e.g. Ref [30], however, this case will not be considered here.

Before discussing the physics associated with the optical delay (which gives rise to dynamical back-action), we briefly divert to a *static* phenomena that is associated with the steady state solutions of the above coupled equations: the mirror bistability [19] and multi-stability [53]. Indeed, as noted earlier, the radiation-pressure-induced bi-stability was observed over two decades ago [19] using a harmonically-suspended mirror. In brief, considering purely the static solutions for the displacement (i.e. $\overline{x}$) of the above set of equations, it becomes directly evident that the equilibrium position of the mechanical oscillator will depend upon the intra-cavity power. Since the latter is again coupled to the mechanical displacement, this leads to a cubic equation for the mirror position $\overline{x}$ as a function of applied power:

$$\frac{\tau^2}{\tau_{ex}}|s|^2 = \frac{cm_{eff}}{\zeta}\Omega_m^2\overline{x}\left(4\tau^2\left(\Delta + \frac{\omega_0}{R}\overline{x}\right)^2 + 1\right) \tag{4}$$

For sufficiently high power, this leads to bi-stable behavior (namely for a given detuning and input power the mechanical position can take on several possible values).

2.2. Modifications due to Dynamic Back-action: Method of Retardation Expansion

The circulating optical power will vary in response to changes in the coordinate "x". The delineation of this response into adiabatic and non-adiabatic contributions provides a starting point to understand the origin of dynamic back-action and its two manifestations. This delineation is possible by formally integrating the above equation for the circulating field, and treating the

#88348 - $15.00 USD Received 8 Oct 2007; revised 7 Dec 2007; accepted 7 Dec 2007; published 10 Dec 2007

term x wihin it as a perturbation. Furthermore, if the time variation of x is assumed to be slow on the time scale of the optical cavity decay time (or equivalently if $\kappa \gg \Omega_m$) then an expansion into orders of retardation is possible. Keeping only terms up to $\frac{dx}{dt}$ in the series expansion, the circulating optical power (and hence the forcing function in the mechanical oscillator equation) can be expressed as follows,

$$P_{cav} = P^0_{cav} + P^0_{cav}\left(\frac{8\Delta\tau^2}{4\tau^2\Delta^2+1}\right)\frac{\omega_0}{R}x - \tau P^0_{cav}\left(\frac{8\Delta\tau^2}{4\tau^2\Delta^2+1}\right)\frac{\omega_0}{R}\frac{dx}{dt} \tag{5}$$

Here the power $P^0_{cav} = \frac{|a|^2}{T_{rt}} = \frac{\tau}{T_{rt}}\frac{2\tau/\tau_{ex}}{4\Delta^2\tau^2+1}|s|^2$ denotes the power in the cavity for zero mechanical displacement. The circulating power can also be written as $P^0_{cav} = \mathscr{F}/\pi \cdot C \cdot |s|^2$, where $C = \frac{\tau/\tau_{ex}}{4\Delta^2\tau^2+1}$ and where $\mathscr{F} = 2\pi\frac{\tau}{T_{rt}}$ denotes the cavity Finesse. The first two terms in this series provide the adiabatic response of the optical power to changes in position of the mirror. Intuitively, they give the instantaneous variations in coupled power that result as the cavity is "tuned" by changes in "x". It is apparent that the $x-$dependent contribution to this adiabatic response (when input to the mechanical-oscillator equation-of-motion through the forcing function term) provides an optical-contribution to the stiffness of the mass-spring system. This so-called *"optical spring"* effect (or *"light induced rigidity"*) has been observed in the context of LIGO [20] and also in microcavities [54]. The corresponding change in spring constant leads to a frequency shift, relative to the unpumped mechanical oscillator eigenfrequency, as given by (where $P = |s|^2$ denotes the input power):

$$\Delta\Omega_m \underset{\kappa\gg\Omega_m}{=} \mathscr{F}^2\frac{8n^2\omega_0}{\Omega_{\mathrm{m}} m_{eff}c^2}C\cdot\left[\frac{2\Delta\tau}{(4\tau^2\Delta^2+1)}\right]P \tag{6}$$

The non-adiabatic contribution in equation5 is proportional to the velocity of the mass-spring system. When input to the mechanical-oscillator equation, the coefficient of this term is paired with the intrinsic mechanical damping term and leads to the following damping rate given by (for a whispering gallery mode cavity of radius R):

$$\Gamma \underset{\kappa\gg\Omega_m}{=} -\mathscr{F}^3\frac{8n^3\omega_0 R}{m_{eff}c^3}C\cdot\left[\frac{16\Delta\tau}{(4\tau^2\Delta^2+1)^2}\right]P \tag{7}$$

This radiation pressure induced damping rate modifies the intrinsic mechanical resonator's loss rate ($\Gamma_m = \Omega_{\mathrm{m}}/Q_m$ where is Q_m the mechanical Q-factor), yielding an (effective) damping rate:

$$\Gamma_{eff} = \Gamma + \Gamma_m \tag{8}$$

In both equations 6 and 7 we have stressed the fact that these expressions are valid only in the weak retardation regime in which $\kappa \gg \Omega_m$. The sign of Γ (and the corresponding direction of power flow) depends upon the relative detuning of the optical pump with respect to the cavity resonant frequency. In particular, a red-detuned pump ($\Delta < 0$) results in a sign such that optical forces augment intrinsic mechanical damping, while a blue-detuned pump ($\Delta > 0$) reverses the sign so that damping is offset (negative damping or amplification). It is important to note that the rate Γ in the weak-retardation regime depends strongly ($\propto \mathscr{F}^3$) on the optical finesse, which has been experimentally verified as discussed in section 4.2. Note also that maximum cooling or amplification rate for a given power occurs when the laser is detuned to the maximum slope of the cavity Lorenzian; these two cases are illustrated in Figure 2. These modifications have been first derived by Braginsky [10] more than 3 decades ago and are termed *dynamic back-action*. Specifically, an optical probe used to ascertain the position of a mirror within an optical resonator, will have the side-effect of altering the dynamical properties of the mirror (viewed as a mass-spring system).

#88348 - $15.00 USD Received 8 Oct 2007; revised 7 Dec 2007; accepted 7 Dec 2007; published 10 Dec 2007

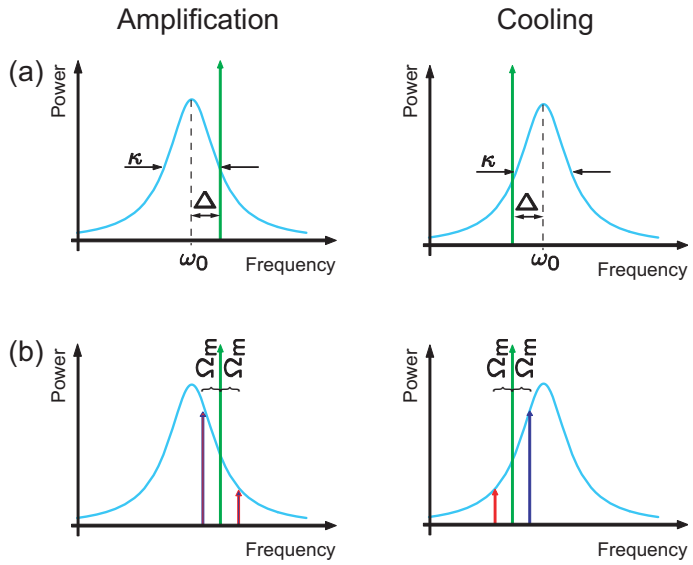

Fig. 2. The two manifestations of dynamic back-action: blue-detuned and red-detuned pump wave (green) with respect to optical mode line-shape (blue) provide mechanical amplification and cooling, respectively. Also shown in the lower panels are motional sidebands (Stokes and anti-Stokes fields) generated by mirror vibration and subsequent Doppler-shifts of the circulating pump field. The amplitudes of these motional sidebands are asymmetric owing to cavity enhancement of the Doppler scattering process.

The direction of power-flow is also determined by the sign of the pump frequency detuning relative to the cavity resonant frequency. Damping (red tuning of the pump) is accompanied by power flow from the mechanical mode to the optical mode. This flow results in cooling of the mechanical mode. Amplification (blue tuning of pump) is, not surprisingly, accompanied by net power flow from the optical mode to the mechanical mode. This case has also been referred to as *heating*, however, it is more appropriately referred to as *amplification* since the power flow in this direction performs work on the mechanical mode. The nature of power flow between the mechanical and optical components of the system will be explored here in several ways, however, one form of analysis makes contact with the thermodynamic analogy of cycles in a Clapeyron or Watt diagram (i.e. a pressure-volume diagram). In the present case – assuming the mechanical oscillation period to be comparable to or longer than the cavity lifetime – such a diagram can be constructed to analyze power flow resulting from cycles of the coherent radiation gas interacting with a movable piston-mirror [55] (see Figure 3). In particular, a plot of radiation pressure exerted on the piston-mirror versus changes in optical mode volume provides a coordinate space in which it is possible to understand the origin and sign of work done during one oscillation cycle of the piston mirror. Considering the oscillatory motion of the piston-mirror at some eigenfrequency Ω_m, then because pressure (proportional to circulating optical power) and displaced volume (proportional to x) have a quadrature relationship (through the dynamic back-action term involving the velocity $\frac{dx}{dt}$), the contour for a PV cycle will encompass a non-zero area, giving the net-work performed during one cycle of mechanical oscillation. Note that the area reduces as the photon lifetime shortens (i.e., as retardation is weakened). Also, the sense in which the PV cycle is traversed is opposite for the two cases of red and blue detuning of the pump (i.e., the area and hence work-done changes sign). For blue detuning, the radiation gas does net work on the piston while the reverse is true for red detuning. The fact that cooling is

#88348 - $15.00 USD Received 8 Oct 2007; revised 7 Dec 2007; accepted 7 Dec 2007; published 10 Dec 2007

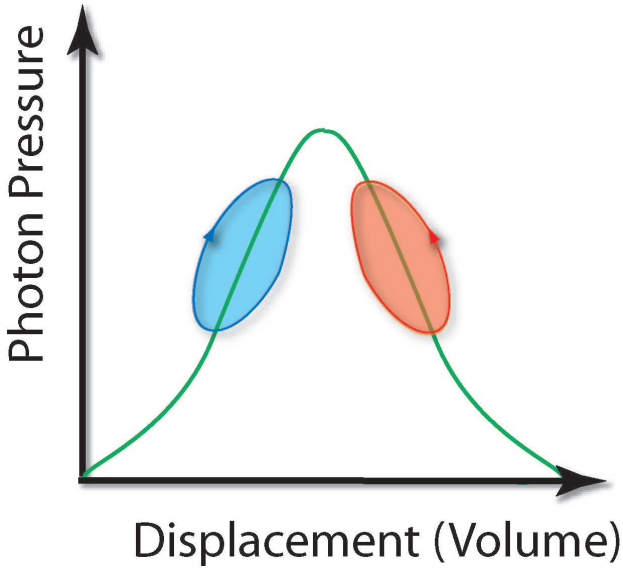

Fig. 3. Work done during one cycle of mechanical oscillation can be understood using a PV diagram for the radiation pressure applied to a piston-mirror versus the mode volume displaced during the cycle. In this diagram the cycle follows a contour that circumscribes an area in PV space and hence work is performed during the cycle. The sense in which the contour is traversed (clockwise or counterclockwise) depends upon whether the pump is blue or red detuned with respect to the optical mode. Positive work (amplification) or negative work (cooling) are performed by the photon gas on the piston mirror in the corresponding cases.

possible for the case of a red detuned pump is the result of both: the sign of work in this case being such that the piston does positive work on the photon gas, and, equally important, that the photon gas (if in a coherent state) provides only quantum, back-action on the piston. This makes the photon gas effectively very cold.

The cooling and amplification processes can also be understood in terms of the creation of stokes and anti-Stokes sidebands [22]. Oscillatory motion of the cavity mirror will create side bands on the probe wave as the circulating optical power is Doppler-shifted by the mirror's motion (or equivalently the expansion and contraction of the whispering gallery in the case of a toroid or disk resonator). As shown in Figure 2, these motional sidebands will have asymmetric amplitudes owing to the fact that the pump wave frequency is detuned from the cavity resonance. The two cases of interest (red and blue detuning) are illustrated in the Figure 2 and produce opposite asymmetry. Intuitively, the sideband that is closer to the cavity resonance has its amplitude resonantly enhanced. This will be rigorously derived in the next section. This asymmetry indicates a net deficit (blue detuned) or surplus (red detuned) of power in the transmitted pump wave. The sideband asymmetry also produces strong amplitude modulation that can be measured as a photocurrent upon detection of the transmitted power from the resonator.

Amplification and damping (i.e. cooling) have been verified experimentally. In particular, a mechanical mode subjected to dynamic backaction through a properly detuned optical pump wave will exhibit a thermal noise spectrum whose line-shape is modified by the presence of added optical damping or amplification (negative damping). In either case, the damping rate will depend in a linear fashion on the coupled optical pump power for fixed pump detuning. Before proceeding with the further development of the theory, it is useful to consider briefly

#88348 - $15.00 USD Received 8 Oct 2007; revised 7 Dec 2007; accepted 7 Dec 2007; published 10 Dec 2007

the measurement of this damping dependence in an actual system (Further details regarding the realization of amplification and cooling will be the subject of sections 4 and 5). Measurement of this behavior is possible by probing the motion of the cavity mirror using the transmitted optical pump wave. If the pump wave is detuned relative to the cavity resonance, it is power-modulated by the resonator since the mechanical motions vary in time the cavity resonance. (Equivalently, the asymmetric motional sidebands on the transmitted pump are detected.) The detected amplitude modulation contains information about the underlying mechanical motion. If, for example, the mirror is undergoing regenerative oscillations (see section 4 below), then spectral analysis of the photocurrent will reveal the oscillation frequency (and even the effective temperature) and measurement of the modulation power can be used to ascertain the mechanical oscillation amplitude. In cases where the mirror is excited only by thermal energy, the spectrally-broad thermal excitation (upon measurement as a photocurrent spectral density) provides a way to observe the oscillator lineshape and thereby determine its linewidth and effective damping rate. If the optical pump wave is weak, this damping rate will reflect the intrinsic loss (intrinsic mechanical $Q_m = \Omega_m/\Gamma_m$) of the mechanical mode. On the other hand, as the probe power is increased, it will modify the damping rate causing the line to narrow (blue detuned) or broaden (red detuned) in accordance with the above model.

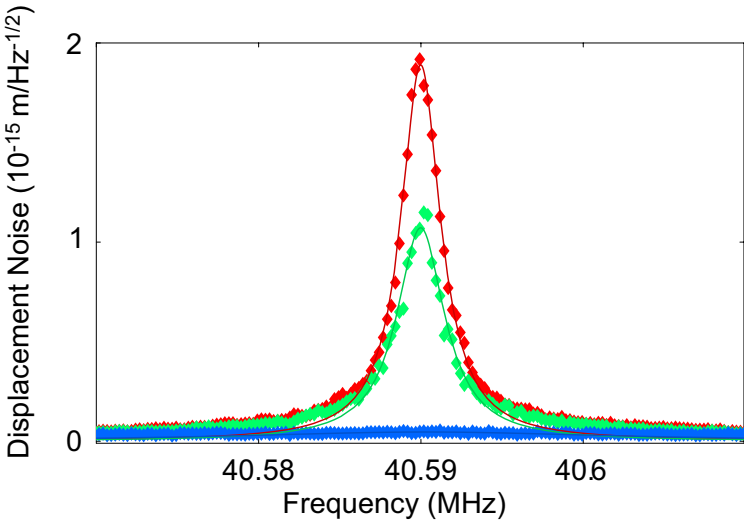

Fig. 4. Dynamics in the weak retardation regime. Experimental displacement spectral density functions for a mechanical mode with eigenfrequency 40.6 MHz measured using three, distinct pump powers for both blue and red pump detuning. The mode is thermally excited (green data) and its linewidth can be seen to narrow under blue pump detuning (red data) on account of the presence of mechanical gain (not sufficient in the present measurement to excite full, regenerative oscillations); and to broaden under red pump detuning on account of radiation pressure damping (blue data).

Figure 4 presents such lineshape data taken using a microtoroid resonator. The power spectral density of the photocurrent is measured for a mechanical mode at an eigenfrequency of 40.6 MHz; three spectra are shown, corresponding to room temperature intrinsic motion (i.e. negligible pumping), mechanical amplification and cooling. In addition to measurements of amplification and damping as a function of pump power (for fixed detuning), the dependence of these quantities on pump detuning (with pump power fixed) can also be measured [28]. Furthermore, pulling of the mechanical eigenfrequency (caused by the radiation pressure mod-

#88348 - $15.00 USD Received 8 Oct 2007; revised 7 Dec 2007; accepted 7 Dec 2007; published 10 Dec 2007

ification to mechanical stiffness) can also be studied [54]. A summary of such data measured using a microtoroid in the regime where $\kappa \gtrsim \Omega_m$ is provided in Figure 5. Both the case of red- (cooling) and blue- (amplification) pump detuning are shown. Furthermore, it can be seen that pump power was sufficient to drive the mechanical system into regenerative oscillation over a portion of the blue detuning region (section of plot where linewidth is nearly zero). For comparison, the theoretical prediction is shown as the solid curve in the plots. Concerning radiation-pressure-induced stiffness, it should be noted that for red-detuning, the frequency is pulled to lower frequencies (stiffness is reduced) while for blue-detuning the stiffness increases and the mechanical eigenfrequency shifts to higher values. This is in dramatic contrast to similar changes that will be discussed in the next section. While in Figure 5 the absolute shift in the mechanical eigenfrequency is small compared to Ω_m, it is interesting to note that it is possible for this shift to be large. Specifically, statically unstable behavior is possible if the total spring constant reaches a negative value. This has indeed been observed experimentally in gram scale mirrors coupled to strong intra-cavity fields by the LIGO group at MIT [29].

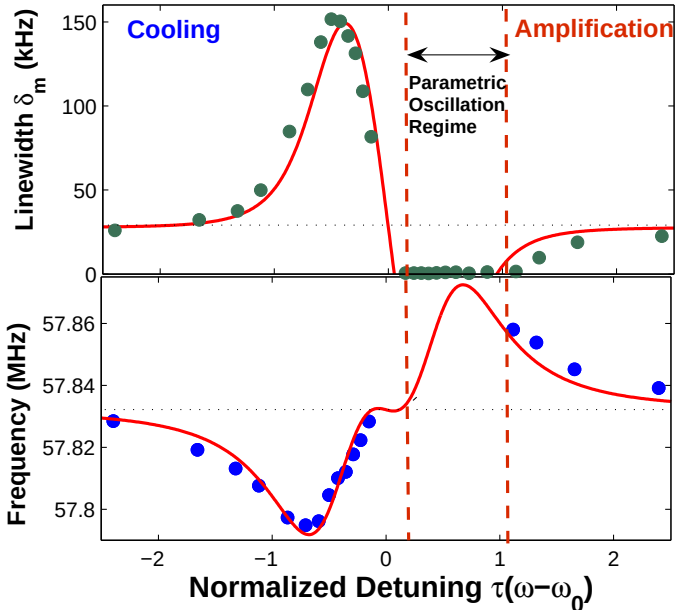

Fig. 5. Upper panel shows mechanical linewidth ($\delta_m = \Gamma_{eff}/2\pi$) and shift in mechanical frequency (lower panel) measured versus pump wave detuning in the regime where $\kappa \gtrsim \Omega_m$. For negative (positive) detuning cooling (amplification) occurs. The region between the dashed lines denotes the onset of the parametric oscillation, where gain compensates mechanical loss. Figure stems from reference [28]. Solid curves are theoretical predictions based on the sideband model (see section 2.2).

While the above approach provides a convenient way to understand the origin of mechanical amplification and damping and their relationship to non-adiabatic response, a more general understanding of the dynamical behavior requires an extension of the formalism. Cases where the mechanical frequency, itself, varies rapidly on the time scale of the cavity lifetime cannot be described correctly using the above model. From the viewpoint of the sideband picture mentioned above, the modified formalism must include the regime in which the sideband spectral

#88348 - $15.00 USD Received 8 Oct 2007; revised 7 Dec 2007; accepted 7 Dec 2007; published 10 Dec 2007

separation from the pump can be comparable to or larger than the cavity linewidth.

2.3. Sideband Formalism

It is important to realize that the derivation of the last section only applies to the case where the condition $\kappa \gg \Omega_m$ is satisfied. In contrast, a perturbative expansion of the coupled mode equations (eqns. 1 and 2) gives an improved description that is also valid in the regime where the mechanical frequency is comparable to or even exceeds the cavity decay rate (where $\Omega_m \gg \kappa$ and is the so called *resolved sideband regime*). The derivation that leads to these results [22,28] is outlined here. For most experimental considerations (in particular for the case of cooling) the quantity $\varepsilon = \frac{x}{2R}$ is very small, and a perturbative expansion of the intracavity field in powers of this parameter is possible, i.e.

$$a \equiv \sum_{n=0}^{\infty} \varepsilon^n a_n \tag{9}$$

Here, the zeroth order perturbation amplitude (a_0) describes the cavity build-up factor in the absence of the opto-mechanical coupling

$$a_0(t) = \frac{i\sqrt{\frac{1}{\tau_{ex}}}}{i\Delta - \frac{1}{2\tau}} s e^{i\omega t} \tag{10}$$

Making the assumption that the mechanical system is undergoing harmonic motion $x(t) = x\cos(\Omega_m t)$, it is possible to solve for the first-order perturbation term:

$$a_1(t) = a_0(t) 2\tau\omega_0 \left(\frac{e^{i\Omega_m t}}{2i(\Delta+\Omega_m)\tau - 1} + \frac{e^{-i\Omega_m t}}{2i(\Delta-\Omega_m)\tau - 1} \right) \tag{11}$$

Inspection shows that this 1st-order term consists of two, independent fields, a frequency up-shifted anti-Stokes sideband ($\omega_{AS} = \omega + \Omega_m$), and a frequency down shifted ($\omega_S = \omega - \Omega_m$) Stokes sideband produced by the harmonic mechanical motion. These fields account for Doppler shifting of the circulating pump field caused by the motion of the mirror or dielectric cavity. The parameter ε is sufficiently small to neglect the higher-order terms in the perturbation. The radiation pressure force acting on the mechanical oscillator in the toroidal (or other whispering gallery mode) cavity is $F_{RP}(t) = \frac{2\pi n}{c}\frac{|a|^2}{T_{rt}}$(and for a Fabry-Perot cavity $F_{RP}(t) = \frac{2}{c}\frac{|a|^2}{T_{rt}}$). Here, T_{rt} is the cavity round trip time and $|a|^2$ and is to 1^{st} order given by $|a|^2 \cong |a_0|^2 + 2\varepsilon\Re(a_0^* a_1)$. The radiation pressure force can now be expressed in terms of *in-phase* and *quadrature* components (with respect to the harmonic displacement, assumed above):

$$F_{RP}(t) = \cos(\Omega_m t) F_I + \sin(\Omega_m t) F_Q \tag{12}$$

Where the in-phase component is given by:

$$F_I(t) = -\varepsilon \frac{4\pi n}{cT_{rt}} \frac{\omega_0 \tau^2/\tau_{ex}}{4\Delta^2\tau^2 + 1} \left(\frac{2(\Delta+\Omega_m)}{4(\Delta+\Omega_m)^2\tau^2 + 1} - \frac{2(\Delta-\Omega_m)}{4(\Delta-\Omega_m)^2\tau^2 + 1} \right) P \tag{13}$$

and the quadrature component takes on the form:

$$F_Q(t) = -\varepsilon \frac{4\pi n}{cT_{rt}} \frac{\omega_0 \tau^2/\tau_{ex}}{4\Delta^2\tau^2 + 1} \left(\frac{2\tau}{4(\Delta+\Omega_m)^2\tau^2 + 1} - \frac{2\tau}{4(\Delta-\Omega_m)^2\tau^2 + 1} \right) P \tag{14}$$

The in-phase part of this force is responsible for changes in rigidity whereas the quadrature part is responsible for changes in the damping factor, which leads to cooling (or amplification).

#88348 - $15.00 USD Received 8 Oct 2007; revised 7 Dec 2007; accepted 7 Dec 2007; published 10 Dec 2007

From the force, the net power (P_m) transferred from the mechanical mode to (or from) the optical mode can be calculated via the relation $\langle P_m \rangle = \langle F_Q(t) \cdot \dot{x} \rangle$ yielding:

$$\langle P_m \rangle = \langle x^2 \rangle \frac{2\pi n}{cT_{rt}} \frac{\omega_0 1/\tau_{ex}}{4\tau^2 \Delta\omega^2 + 1} \frac{\Omega_m}{2R} \left(\frac{2\tau}{4(\Delta+\Omega_m)^2\tau^2+1} - \frac{2\tau}{4(\Delta-\Omega_m)^2\tau^2+1} \right) P \qquad (15)$$

This quantity can be recognized as the difference in intra-cavity energy of anti-Stokes and Stokes modes, i.e. $\langle P_m \rangle = (|a_{AS}|^2 - |a_S|^2)/T_{rt}$, as expected from energy conservation considerations. Consequently, this analysis reveals how the mechanical mode extracts (amplification) or loses energy (cooling) to the optical field, despite the vastly different frequencies. Cooling or amplification of the mechanical mode thus arises from the fact that the two side-bands created by the harmonic mirror motion are *not equal* in magnitude, due to the detuned nature of the excitation (see Figure 2). In the case of cooling, a red detuned laser beam will cause the system to create more anti-Stokes than Stokes photons entailing a net power flow from the mechanical mode to the optical field. Conversely, a blue-detuned pump will reverse the sideband asymmetry and cause a net power flow from the optical field to the mechanical mode, leading to amplification. We note that in the case of cooling, the mechanism is similar to the cooling of atoms or molecules inside an optical resonator via "coherent scattering" as theoretically proposed [56] and experimentally observed [57]. From the power calculation, the cooling or mechanical amplification rate $\Gamma = \frac{\langle P_m \rangle}{m_{eff}\Omega_m^2 \langle x^2 \rangle}$ can be derived and expressed as:

$$\Gamma = -\mathscr{F}^2 \frac{8n^2\omega_0}{\Omega_{\mathrm{m}} m_{eff} c^2} C \cdot \left(\frac{1}{4(\Delta-\Omega_m)^2\tau^2+1} - \frac{1}{4(\Delta+\Omega_m)^2\tau^2+1} \right) P \qquad (16)$$

Here the finesse $\mathscr{F}$ has been introduced (as before) as well as the previously introduced dimensionless coupling factor $C = \frac{\tau/\tau_{ex}}{4\Delta^2\tau^2+1}$ which takes on a value between 0..1. Analysis of the above formula allows derivation of the optimum detuning, for which the cooling or amplification rate is maximum. Note that in the limit of $\kappa \gg \Omega_m$ one recovers the result of the previous section (equation 7), as

$$\lim_{\Omega_m \to 0} \frac{1}{2\Omega_m} \left(\frac{1}{4(\Delta-\Omega_m)^2\tau^2+1} - \frac{1}{4(\Delta+\Omega_m)^2\tau^2+1} \right) = \frac{8\Delta\tau^2}{\left(4\Delta^2\tau^2+1\right)^2} \qquad (17)$$

Hence, as noted before, in the weak retardation regime, the maximum cooling (or amplification) rate for a given power occurs when the laser is detuned to the maximum slope of the cavity Lorenzian; i.e. $|\Delta| = \kappa/2$, in close analogy to Doppler cooling [6] in Atomic Physics. On the other hand, in the resolved sideband regime optimum detuning occurs when the laser is tuned either to the lower or upper "motional" sideband of the cavity, i.e. $\Delta = \pm\Omega_m$. This behavior is also shown in Figure 6. The above rate, as noted earlier, modifies the dynamics of the mechanical oscillator. In the case of amplification (blue detuned pump) it offsets the intrinsic loss of the oscillator and overall mechanical damping is reduced. Ultimately, a "threshold condition" in which mechanical loss is completely offset by gain occurs at a particular pump power. Beyond this power level, regenerative mechanical oscillation occurs. This will be studied in section 4 below.

For red detuning, the oscillator experiences enhanced damping. Beyond the power flow analysis provided above, a simple classical analysis can also be used to understand how such damping can result in cooling. Specifically, in the absence of the laser, the mean energy (following from the equation for x) obeys $\frac{d}{dt}\langle E_m \rangle = -\Gamma_m \langle E_m \rangle + k_B T_R \Gamma_m$, implying that the mean steady state energy is given by the reservoir temperature $\langle E_m \rangle = k_B T_R$. When considering the modifications to this equation resulting from back-action damping, an additional loss term appears in

#88348 - $15.00 USD Received 8 Oct 2007; revised 7 Dec 2007; accepted 7 Dec 2007; published 10 Dec 2007

the equation for the average energy:

$$\frac{d}{dt}\langle E_m\rangle = -(\Gamma_m+\Gamma)\langle E_m\rangle + k_B T_R \Gamma_m \tag{18}$$

Note that within this classical model, the cooling introduced by the laser is what has been described by some authors [32] as "*cold damping*": the laser introduces a damping without introducing a modified Langevin force (in contrast to the case of intrinsic damping). This is a key feature and allows the enhanced damping to reduce the mechanical oscillator temperature, yielding as a final effective temperature for the mechanical mode under consideration:

$$T_{eff} \cong \frac{\Gamma_m}{\Gamma_m+\Gamma} T_R \tag{19}$$

It deserves notice that the above formula predicts that arbitrarily low temperatures can be attained. As discussed later, the laser damping also introduces a small noise term, due to the quantum nature of light, which adds a further Langevin force to previous equations. This will be considered in the last section and is shown to provide the ultimate cooling limit of this technique. Moreover, it is noted that the above formula is only valid [48, 49] as long as $\Gamma \ll \kappa$ and as $\frac{\Gamma_m}{\Gamma_m+\Gamma} > \frac{1}{Q_m}$.

For completeness, the in-phase component of the radiation pressure force is also investigated. This component of the force causes a change in the mechanical oscillator's rigidity, and its adiabatic contribution is the well-known optical spring effect described earlier. Specifically, the change in mechanical resonance frequency (from its intrinsic value) is given by:

$$\Delta\Omega_m = \mathscr{F}^2 \frac{8n^2\omega_0}{\Omega_{\mathrm{m}} m_{eff} c^2} C\tau \cdot \left(\frac{\Delta-\Omega_m}{4(\Delta-\Omega_m)^2\tau^2+1} + \frac{\Delta+\Omega_m}{4(\Delta+\Omega_m)^2\tau^2+1} \right) P \tag{20}$$

Note that in the regime where the mechanical frequency is comparable to, or exceeds the cavity decay rate it's behavior is quite different from that described earlier for the conventional adiabatic case; and was only recently observed experimentally [28]. As noted earlier, in the adiabatic regime, the mechanical frequency is always downshifted by a red-detuned laser (i.e. a reduced rigidity). However, when $\Omega_m > 1/2 \cdot \kappa$ an interesting phenomena can occur. Specifically, when the pump laser detuning is relatively small, the mechanical frequency shift is opposite in sign to the conventional, adiabatic spring effect. The same behavior can occur in the case of amplification ($\Delta > 0$). Furthermore, a pump detuning exists where the radiation-pressure induced mechanical frequency shift is zero, even while the damping/amplification rate is non-zero. The latter has an important meaning as it implies that the entire radiation pressure force is *viscous* for red detuning, contributing only to cooling (or to amplification for blue detuning). Figure 6 shows the attained cooling/amplification rate (as a contour plot) for fixed power and mechanical oscillator frequency as a function of normalized optical cavity decay rate and the normalized laser detuning (normalized with respect to $\Delta_{opt} = \sqrt{\Delta^2+\kappa^2/4}$). Both the unresolved and resolved-sideband regimes are delineated in the plot. Evidently, the highest cooling/amplification rates are achieved in the resolved sideband regime, provided the pump laser is detuned to $+\Omega_m$ or $-\Omega_m$ (i.e. corresponding to the cavities lower and upper motional sideband).

An important feature of cooling and amplification provided by dynamic back-action is the high level of mechanical spectral selectivity that is possible. Since, the cooling/amplification rates depend upon asymmetry in the motional sidebands, the optical line-width and pump laser detuning can be used to select a particular mechanical mode to receive the maximum cooling or amplification. In effect, the damping/amplification rates shown above have a spectral shape (and spectral maximum) that can be controlled in an experimental setting as given by horizontal

#88348 - $15.00 USD Received 8 Oct 2007; revised 7 Dec 2007; accepted 7 Dec 2007; published 10 Dec 2007

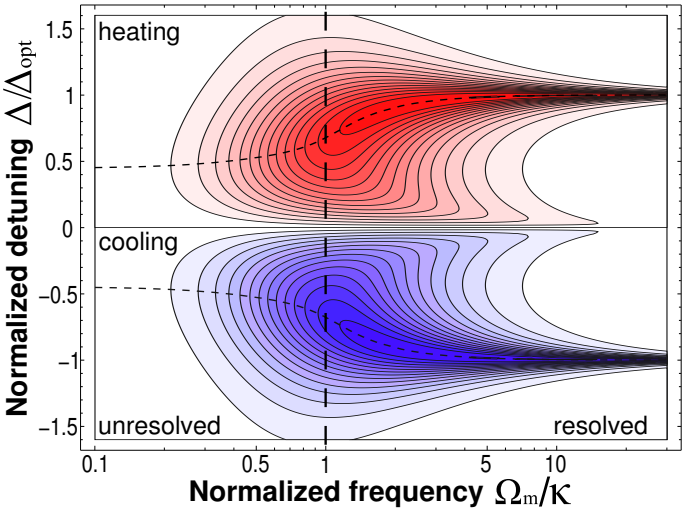

Fig. 6. The mechanical amplification and cooling rate as a function of detuning and normalized mechanical frequency. Also shown is the optimum amplification and cooling rate for fixed frequency (dotted lines). In the simulation, pump power and cavity dimension are fixed parameters.

cuts of Figure 6. This feature is important since it can provide a method to control oscillation frequency in cases of regenerative oscillation on the blue detuning of the pump. Moreover, it restricts the cooling power to only one or a relatively small number of mechanical modes. In cases of cooling, this means that the overall mechanical structure can remain at room temperature while a target mechanical mode is refrigerated.

The full-effect of the radiation-pressure force (both the in-phase component, giving rise to a mechanical frequency shift, and the quadrature-phase component which can give rise to mechanical amplification/cooling) were studied in a "detuning series", as introduced in the last section. The predictions made in the $\Omega_m > 0.5\kappa$ regime have been verified experimentally as shown in Figure 7. Specifically, the predicted change in the rigidity dependence of the oscillator on detuning was experimentally observed as shown in Figure 7 and is in excellent agreement with the theoretical model (solid red line). Keeping the same sample but using a different optical resonance with a line-width of 113 MHz (57.8 MHz mechanical resonance), the transition back to a pure increasing and decreasing mechanical frequency shift in the cooling and amplification regimes was observed as also shown in the preceding section, again confirming the validity of our theoretical model based on the motional sidebands.

3. Optomechanical Coupling and Displacement Measurements

3.1. Mechanical Modes of Optical Microcavities

The coupling of mechanical and optical modes in a Fabry Perot cavity with a suspended mirror (as applying to the case of gravitational wave detectors) or mirror on a spring (as in the case of a cantilever) is easily seen to result from momentum transfer upon mirror reflection and can be described by a Hamiltonian formalism [50]. It is, however, important to realize that radiation pressure coupling can also occur in other resonant geometries: notably in the class of optical-whispering-gallery-mode (WGM) microcavities such as microspheres [58], microdisks [59] and microtoroids [60] (see Figure 8). Whereas in a Fabry Perot cavity the momentum transfer occurs along the propagation direction of the confined photons [10], the mechanism of

#88348 - $15.00 USD Received 8 Oct 2007; revised 7 Dec 2007; accepted 7 Dec 2007; published 10 Dec 2007

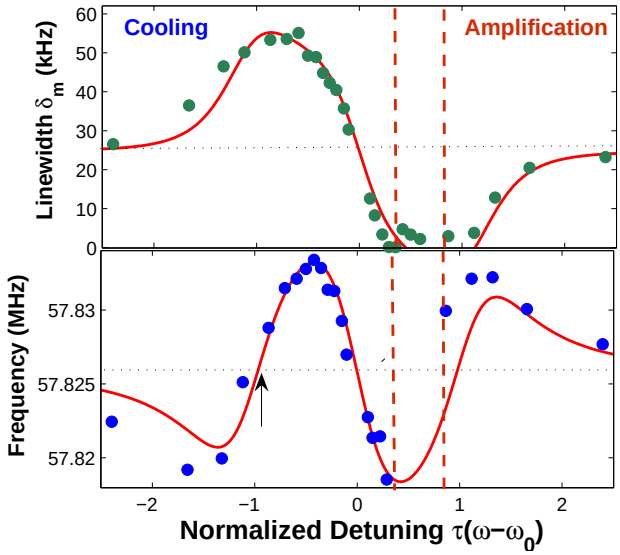

Fig. 7. Dynamics in the regime where $\Omega_m > \kappa$ as reported in reference [28]. Upper panel shows the induced damping /amplification rate ($\delta_m = \Gamma_{eff}/2\pi$) as a function of normalized detuning of the laser at constant power. The points represent actual experiments on toroidal microcavities, and the solid line denotes a fit using the sideband theoretical model (Equations 16 and 20). Lower panel shows the mechanical frequency shift as a function of normalized detuning. Arrow denotes the point where the radiation pressure force is entirely viscous causing negligible in phase, but a maximum quadrature component. The region between the dotted lines denotes the onset of the parametric instability (as discussed in section 4). Graph stems from reference [28].

radiation pressure coupling in a whispering gallery mode cavity occurs normal to the optical trajector [22–24]. This can be understood to result from momentum conservation of the combined resonator-photon system as photons, trapped within the whispering gallery by continuous total-internal reflection, execute circular orbits. In particular, their orbital motion necessitates a radial radiation pressure exerted onto the cavity boundary. The latter can provide coupling to the resonator's mechanical modes.

While the mechanical modes of dielectric microspheres are well known and described by analytic solutions (the Lamb theory), numerical finite-element simulations are required to calculate the frequency, as well as strain and stress fields, of more complicated structures (exhibiting lower symmetry) such as micro-disks and micro-toroids. In the case of a sphere [61], two classes of modes exist. Torsional vibrations exhibit only shear stress without volume change, and therefore no radial displacement takes place in these modes. Consequently these modes cannot be excited using radiation pressure, which relies upon a change in the optical path length (more formally, these modes do not satisfy the selection rule of opto-mechanical coupling, which requires that the integral of radiation pressure force and strain does not vanish along the optical trajectory). In contrast, the class of modes for which volume change is present is referred to as spheroidal modes. An example of this type of mode is the radial breathing mode of a microsphere. In the case of a toroid, this mode's equivalent is shown in Figure 8 and exhibits a radially-symmetric, mechanical displacement of the torus. Note that in a rotationally symmetric WGM microcavity, efficient opto-mechanical coupling requires that the mechanical

#88348 - $15.00 USD Received 8 Oct 2007; revised 7 Dec 2007; accepted 7 Dec 2007; published 10 Dec 2007

modes exhibit the same rotational symmetry (i.e. satisfy the opto-mechanical selection rule). Deviations may occur in cases where the symmetry is lowered further due to eccentricities in the shape of the resonator, and in such cases excitation of modes of lowered symmetry is possible. Excitation of eccentricity split modes has been observed in microtoroids [62], but these cases are not considered here for the sake of simplicity.

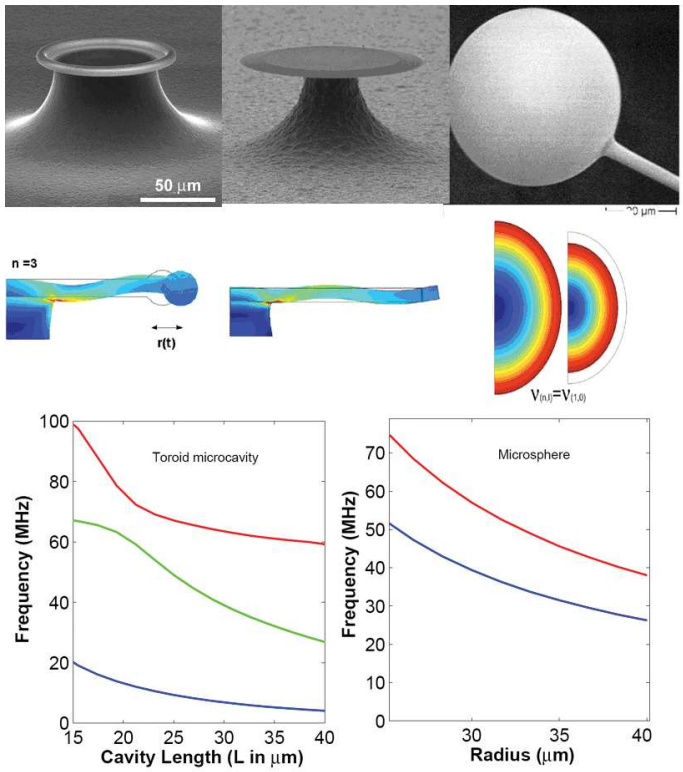

Fig. 8. Upper panel: SEM images and mechanical modes of several types of whispering gallery mode microcavities: toroid microcavities [60] microdisks [59] and microspheres [58]. Also shown are the stress and strain field in cross section of the fundamental radial breathing modes, which include radial dilatation of the cavity boundary. Lower panel: the dispersion diagram for the lowest lying, rotationally symmetric mechanical modes for a toroid (as a function of its undercut) and for a microsphere (as a function of radius).

A unique aspect of the micro-cavities, in contrast to other optomechanical platforms, is that their fundamental mechanical breathing modes can exhibit high mechanical frequency. The radial breathing mode of a $60-$micron-diameter micro-sphere is equal to ~ 55 MHz, and, indeed, microwave-rate regenerative opto-mechanical oscillation has been achieved in spheroidal microresonators [63]. This feature is important in the context of ground-state cooling as described later. It is also potentially important should these devices find applications as high-frequency oscillators. Another important aspect of the mechanical modes in these structures is the level of dissipation, which is governed by several loss mechanisms (clamping losses, thermoelastic losses, etc.). While detailed understanding of dissipation in dielectric microcavities is presently being established, quality factors as high as $50,000$ have been observed at 50 MHz and room

#88348 - $15.00 USD Received 8 Oct 2007; revised 7 Dec 2007; accepted 7 Dec 2007; published 10 Dec 2007

temperature, comparing favorably with the best nano-mechanical resonators [16] to date at low temperatures.

While the micro-mechanical modes coexist within the same physical structure as the optical whispering gallery modes, it is important to note that there is high level of spatial separation between the modes of these physical systems. In fact, the optical whispering gallery confines optical energy to the extreme periphery of the device, while the mechanical mode impacts the entire structure. It is therefore possible to affect changes in the mechanical Q and eigenfrequency spectrum by introduction of micro-mechanical probes without affecting in any way the optical properties of the resonator. This feature can provide additional ways to investigate the physics of these devices. For example, a micro-mechanical probe, when scanned across the surface of a microtoroid, is found to modify the eigenfrequency of a mechanical mode in proportion to the amplitude-squared of the mode function. By measuring the mechanical eigenfrequency during such a scan (using the optical probe technique described above), the underlying mechanical mode can be "imaged." Figure 9 provides images taken of both a fundamental and first-excited mode in a microtoroid.

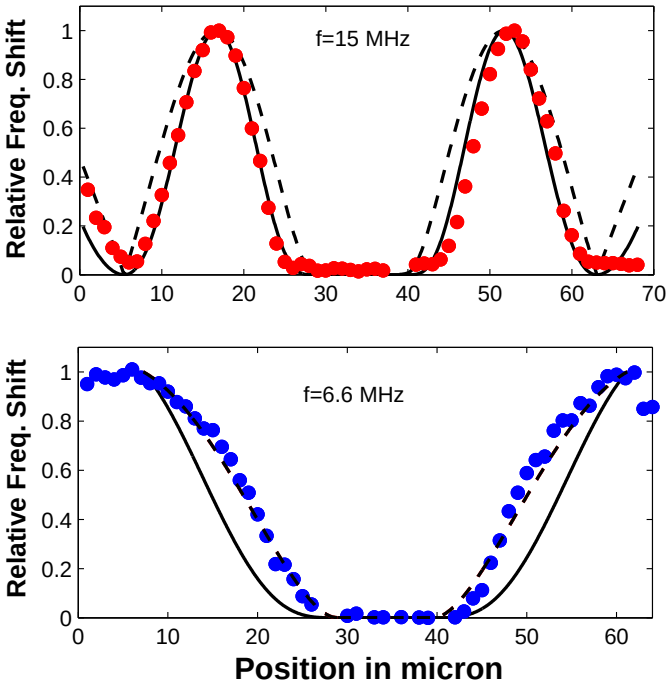

Fig. 9. Scanning probe microscopy of the two lowest lying micro-mechanical resonances of a toroid microcavity. Lower graph: The normalized mechanical frequency shift for the first mode as a function of position. Upper graph: The normalized frequency shift for the second mechanical mode as a function of scanned distance across the toroid. Superimposed is the scaled amplitude (solid line) and the amplitude squared (dotted line) of the mechanical oscillator modes obtained by finite element simulation of the exact geometry parameters (as inferred by SEM).

3.2. Measuring the Opto-mechanical Response

The mechanical properties of whispering gallery mode microcavities can be probed by coupling resonant laser radiation into the microcavities using tapered optical fibers [64]. Such probing

#88348 - $15.00 USD Received 8 Oct 2007; revised 7 Dec 2007; accepted 7 Dec 2007; published 10 Dec 2007

will detect mirror or cavity motion as a modulation in the power transmitted past the resonator. This modulation can, in turn, be measured as a photocurrent upon detection with a photodiode. The continuous, optical probe wave, itself, can also be used to affect changes in the mirror dynamics via the back-action effect. A schematic of the experiment, which can be used to study optomechanical phenomena, is shown in the Figure 10 below. It consists of a continuous-wave pump laser (here, a 965−nm diode laser) which is coupled into a standard, single-mode optical fiber. This fiber enters the experimental chamber, where it also contains a tapered region used to enable evanescent coupling between the tapered fiber and various types of microcavities. The output fiber is connected to different analysis instruments, including an electrical spectrum analyzer and oscilloscope. Note that moreover locking electronics is used to ensure operation at a fixed detuning.

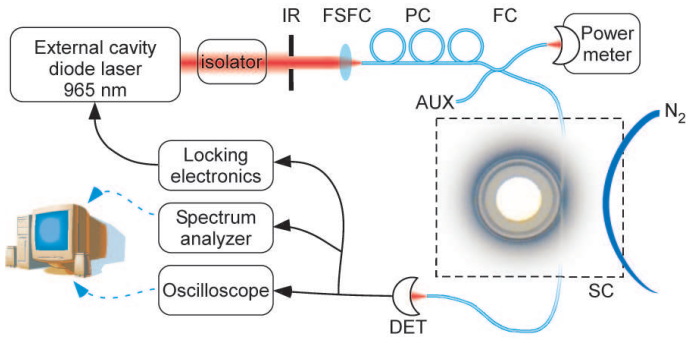

Fig. 10. Experimental setup for the observation of cavity cooling or amplification of a mechanical oscillator. All relevant data from the electronic spectrum analyzer and the oscilloscope are transferred to a computer controlling the experiment. More details in the text. IR: iris, FSFC: free-space to fibre coupler, PC: fibre polarization controller, FC: fibre coupler, AUX: auxiliary input, SC: sealed chamber, DET: fast photoreceiver.

3.3. Displacement Sensitivity

Both the damping rate as well the effective temperature of a mechanical mode are observed by measuring the calibrated displacement noise spectra as a function of power. Despite their small amplitude, these thermally excited oscillations are readily observable in the transmitted light. Indeed, optical interferometers are among the most sensitive monitors for displacement. For quantum-noise-limited homodyne detection the shot noise limited displacement sensitivity of a cavity opto-mechanical system is given by:

$$\delta x_{\min} \cong \frac{\lambda}{8\pi\mathscr{F}\sqrt{\eta P/\hbar\omega}} \tag{21}$$

For numbers typical of the toroidal microcavity work ($\mathscr{F} \approx$40000, $\eta \approx 0.5, P \approx 1\ \mu$W, $\lambda =$ 1064 nm) this implies a displacement sensitivity of $\delta x_{\min} \cong 5 \cdot 10^{-19}\,\mathrm{m}/\sqrt{\mathrm{Hz}}$. Note that this is a remarkably low level, which has been experimentally achieved in a similar approach at the LKB [36]. Interestingly, it is in principle, even sufficient to detect the zero point motion $\delta x_{\min} \cong 5 \cdot 10^{-16}\,\mathrm{m}$ within a 1 kHz resolution bandwidth. In practice, however, such a value can only be achieved in cases where true quantum-limited-readout is present, necessitating lasers which operate with quantum limited amplitude and phase noise, i.e., do not have excess classical noise in either of the two quadratures (the latter is the case of Nd:YAG Lasers for frequencies above ca. 1 MHz). For the experimental measurements described [28] herein the actual displacement

#88348 - $15.00 USD Received 8 Oct 2007; revised 7 Dec 2007; accepted 7 Dec 2007; published 10 Dec 2007

sensitivity did not achieve this level owing to the fact that the diode lasers exhibited excess phase noise, and limited the sensitivity to a value of about $\delta x_{\min} \cong 5 \cdot 10^{-18}\,\mathrm{m}/\sqrt{\mathrm{Hz}}$. Recent work, however, has also obtained higher sensitivity by employing low noise lasers [47]. A typical calibrated and broadband displacement spectrum that can be attained with diode lasers is shown in Figure 11. It reveals several mechanical modes, which can be accurately assigned via finite element modeling.

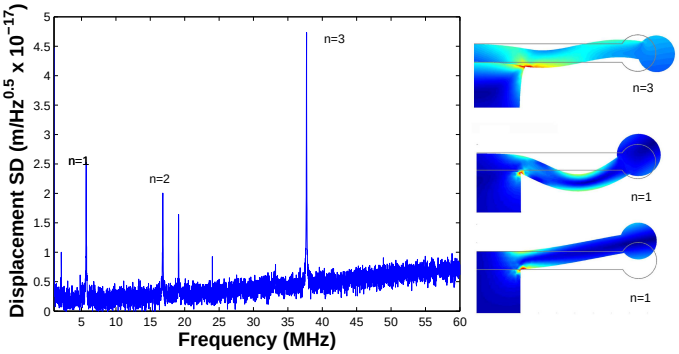

Fig. 11. Calibrated [47] displacement spectral density as measured by the setup shown in Figure 10. The peaks denote different mechanical eigenmodes of the toroidal microcavity. The probe power is sufficiently weak such that the mechanical modes amplitude is dominated by Brownian motion at room temperature and backaction effects are negligible. Cross-sectional representations of the $n = 1,2,3$ modes and their corresponding spectral peaks are also given as inferred by finite element simulations.

4. Blue Detuning: Mechanical Amplification and Oscillation

4.1. Threshold and Mode Selection Mechanisms

Regenerative oscillation occurs in the case of a blue-detuned optical pump wave and at pump power levels above a threshold pump power (P_{thresh}). The oscillation threshold occurs when mechanical amplification (gain) balances mechanical loss. By equating the expression for the mechanical amplification rate Γ of a specific mechanical mode (equation 16) to its intrinsic loss $(\Gamma_m = \Omega_m/Q_m)$, the following expression for threshold optical pump power results.

$$P_{thresh} = \frac{\Omega_m^2}{Q_m}\frac{m_{eff}c^2}{\omega_0 \mathscr{F}^2 8n^2 C}\cdot\left(\frac{1}{4(\Delta-\Omega_m)^2\tau^2+1}-\frac{1}{4(\Delta+\Omega_m)^2\tau^2+1}\right)^{-1} \tag{22}$$

In the case of weak retardation $(\kappa \gg \Omega_m)$ this result simplifies to:

$$P_{thresh} \underset{\kappa\gg\Omega_m}{=} \frac{\Omega_m}{Q_m}\frac{m_{eff}c^3}{\mathscr{F}^3 8n^3 RC\omega_0}\left(\frac{16\Delta\tau}{\left(4\tau^2\Delta^2+1\right)^2}\right)^{-1} \tag{23}$$

It is worth noting that even though cooling does not exhibit a similar threshold condition, the above condition, when expressed for the case of red-detuning of the pump wave, gives the condition in which the radiation pressure cooling rate equals the heating rate of the mechanical mode. As such, a factor of $\times 2$ in temperature reduction (cooling) already requires that parametric oscillation is observable for the corresponding blue detuning.

#88348 - $15.00 USD Received 8 Oct 2007; revised 7 Dec 2007; accepted 7 Dec 2007; published 10 Dec 2007

An important feature of the mechanical gain is its dependence with respect to the mechanical eigen-frequency (i.e, the gain spectum). Mechanical modes whose eigenfrequencies fall near the peak of this curve have the lowest threshold pump power for oscillation. The general shape of this curve can be inferred from Figure 6, which shows a contour plot of both the gain and the cooling rate versus the normalized mechanical eigenfrequency and the normalized detuning. As noted earlier above, horizontal slices of this plot give the gain (or cooling rate) spectral shapes. Experimental control of the spectral peak of the gain (cooling rate) is obviously important since it determines which mechanical modes oscillate or receive maximum cooling. The contour of maximum gain appears as a dashed contour in the plot (likewise there is a corresponding contour for maximum cooling rate). The unresolved sideband case (case of weak retardation) in the figure provides an convenient physical limit in which to illustrate one form of spectral control. In this case, as noted before, the contour of maximum gain (cooling) occurs when the pump wave is detuned to the half-max position of the optical lineshape function (cf. the vertical axis value of the contour in unresolved sideband regime). The maximum mechanical gain increases along this contour as the parameter $\Omega_{\mathrm{m}}/\kappa$ increases towards 0.5 and then diminishes beyond this value (for pump-wave detuning fixed). (Beyond this value, even somewhat before it is reached, the pump detuning must be adjusted continuously in concert with increases in $\Omega_{\mathrm{m}}/\kappa$ to remain on the contour of maximum gain. This is a result of transition into the sideband resolved regime as described earlier). This can be understood in the context of the motional side band (Stokes/anti-Stokes waves) description provided earlier (see Figure 2). Specifically, the case of a pump wave detuned to the half-max point is diagrammed in Figure 12 for three values of the parameter $\Omega_{\mathrm{m}}/\kappa$ ($<,=,>0.5$). The corresponding side-band configuration in each of these cases is also illustrated for comparison. Since mechanical gain is largest when the sideband asymmetry is maximum, the intermediate case of $\Omega_{\mathrm{m}}/\kappa = 0.5$ will exhibit maximum gain in the scenario depicted in Figure 12. Through adjustments of the optical mode line-width (as can be done by controlling waveguide loading of the microresonator) an optimum $\Omega_{\mathrm{m}}/\kappa$ can therefore be set experimentally. This method has, in fact, been used to provide targeted oscillation of mechanical modes (even into the microwave regime) through control of optical waveguide loading. It is important to note however that the above considerations assume a constant normalized detuning. If the detuning is allowed to vary as well, maximum cooling or amplification rates always occurs in the resolved sideband regime, when the detuning equates to $\Delta = \pm\Omega_{\mathrm{m}}$ (cf. Figure 6). The inherent advantages of this regime are that it enables a higher level of asymmetry in the side bands. As described in the next section, side-band asymmetry takes on even greater significance in the context of ground state cooling.

4.2. Threshold dependence on optical Q and mechanical Q

There are several additional features of the threshold equation that are worth noting. First, it exhibits a classic inverse dependence on mechanical Q. This is a signature for any regenerative system. Second, in the unresolved sideband regime, the threshold exhibits an inverse-cubic dependence on the optical Q factor (and correspondingly also Finesse). The measurement of these inherent dependences provides further evidence of the underlying nature of the interaction. Measurement of the threshold is straightforward and involves monitoring the photocurrent of the detected transmission either in the time domain or on a spectrum analyzer (as described earlier). The amplitude of oscillations at a particular mechanical eigen-frequency will exhibit a "threshold knee" when plotted versus the coupled optical pump power. This knee is an easily measurable feature and one example is provided in Figure 13. It is important to note that despite the small amplitude of the mechanical oscillations (cf. Fig. 13), the modulation index of the transmitted optical pump wave is very high (even 100%).

The first observation of radiation pressure mechanical amplfication and parametric oscilla-

#88348 - $15.00 USD Received 8 Oct 2007; revised 7 Dec 2007; accepted 7 Dec 2007; published 10 Dec 2007

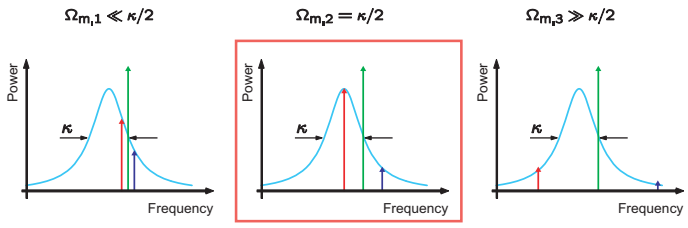

Fig. 12. Back-action tuning for mode selection with a fixed laser detuning corresponding to $\Delta = \kappa/2$. The target mode that receives maximum gain (or optimal cooling for $\Delta = -\kappa/2$) can be controlled by setting the cavity linewidth to produce maximum sideband asymmetry for that particular mechanical mode. In this schematic, three mechanical modes (having frequencies $\Omega_{m,i}$, $i = 1,2,3$) interact with an optical pump, however, in the present scenario only the intermediate mode experiences maximum gain (or cooling) since its sideband asymmetry is maximal (since $\Omega_{m,2}/\kappa = 0.5$). It is important to note however, that if the laser detuning is allowed to vary as well, the highest frequency mode would experience the the largest gain if $\Delta = \Omega_{m,2}$ was chosen.

tion, was made in toroidal micro-cavities [22–24]. The setup employed a tapered optical fiber coupling such that optical loading could be controlled during the experiment. This enabled control of the optical linewidth as described above to effect control of the specific mechanical mode designated for oscillation. When exciting the cavity using a blue-detuned laser pump, an oscillatory output of the cavity could be observed, indicative of the excitation of mechanical modes. The oscillation is readily observable in microtoroids with threshold values in the microwatt range. Indeed, by using typical parameters in the above threshold equation ($\mathscr{F} \approx 10^5$, $m_{eff} \approx 10^{-11}$ kg, $Q_m \approx 10^4$) a threshold in the range of a few micro-Watts is predicted (which is even below the threshold for Raman [65] and parametric oscillations [66]). The fact that this process can be observed in a reproducible manner allows probing of fundamental metrics of these phenomena including the above-noted mechanical and optical Q-dependences.

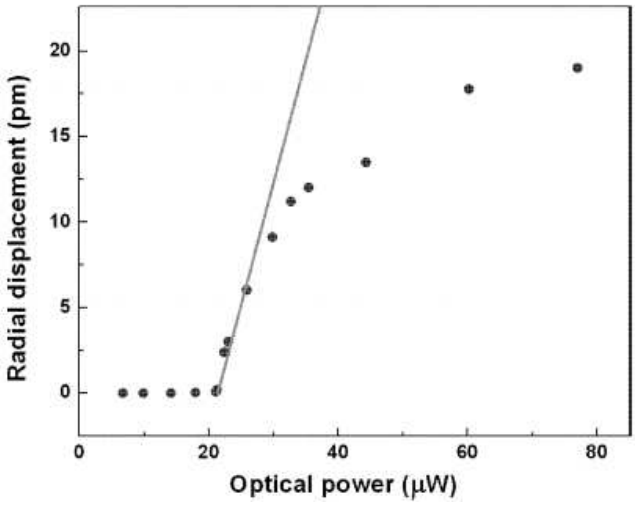

Fig. 13. Regenerative oscillation amplitude plotted versus pump power. The threshold knee is clearly visible. In this case a threshold of 20 μW is observed. Figure from reference [23].

#88348 - $15.00 USD Received 8 Oct 2007; revised 7 Dec 2007; accepted 7 Dec 2007; published 10 Dec 2007

Measurement of the dependence of the parametric oscillation threshold on the mechanical Q is shown in Figure 14. In this experiment, first reported in ref [22], the mechanical $Q-$factor was varied while the optical Q factor was left unchanged. In a variation on the mechanical probing technique described above to provide image scans of the mechanical mode, a micro-probe, in the form of a sharp silica fiber tip, was brought into contact, at a fixed position, with the interior of the microcavity. This caused dissipative coupling of the mechanical mode, decreasing its value from an initial, room temperature and ambient pressure $Q-$value of 5000 to below 50. As noted above, while the mechanical probe modifies the Q (and weakly, the eigen-frequency) of the mechanical mode, it has no effect on the optical performance of the whispering gallery. Therefore, by using this method, the dependence of threshold on mechanical Q can be probed in a nearly ideal way. Gradual change could be induced by variation of the tip pressure. Figure 14 shows the result of this measurement for the $n = 1$ flexural mode. As is evident, there is excellent agreement with the theoretical prediction.

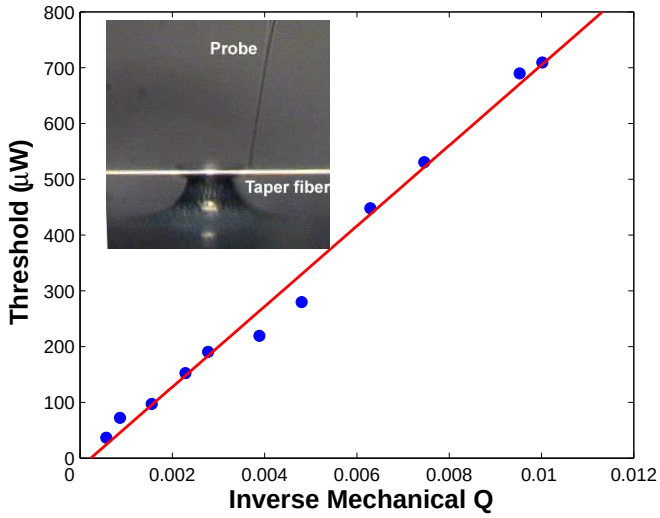

Fig. 14. Main figure: The observed threshold for the parametric oscillation (of an $n = 1$ mode) as a function of inverse mechanical quality factor. In the experiment, variation of Q factor was achieved by placing a fiber tip in mechanical contact with the silica membrane, which thereby allowed reduction of the mechanical Q (cf. inset). The mechanical mode was a 6 MHz flexural mode.

Next, we examine the measured oscillation threshold dependence on the optical Q factor. To illustrate behavior occurring in the sideband resolved and unresolved regimes two mechanical modes were measured: a fundamental $(n = 1)$ at 4.4 MHz and a third-order mode $(n = 3)$ at 49 MHz. The optical Q factor was adjusted by exciting different radial and transverse optical modes. For lower optical Q, wherein the mechanical oscillation frequency falls within the cavity bandwidth (i.e. the adiabatic regime), a rapid dependence $1/Q^3$ is observed, which is in agreement with the threshold equation (i.e. $P_{thresh} \propto 1/\mathscr{F}^3$ cf. equation 23). However, the scaling of threshold changes once a transition from the unresolved (weak retardation) to the resolved sideband limit occurs. Indeed, for $\Omega_m \gtrsim \kappa$, the threshold dependence on optical Q (and Finesse) weakens and eventually approaches an asymptotic value for $\Omega_m \gg \kappa$. The deviation from the cubic dependence is indeed observed experimentally as shown in Figure 15. The solid line in the figure is a prediction based on the threshold equation 22 with effective mass as an adjustable parameter (where optimum detuning is assumed, and optimum coupling for each

#88348 - $15.00 USD Received 8 Oct 2007; revised 7 Dec 2007; accepted 7 Dec 2007; published 10 Dec 2007

optical Q value). The inset of Figure 15 shows the threshold behavior for the $n = 3$ mechanical mode for which $\Omega_m \gtrsim \kappa$ is satisfied over the entire range of Q values. As expected, a much weaker dependence on optical Q-factor is found as predicted theoretically. Direct comparison with the $n = 1$ mode data shows that oscillation on the $n = 3$ mode is preferred for lower optical Qs. Indeed, preference to the $n = 3$ mode was possible by increased waveguide loading of the microcavity in agreement with theory. The solid curve in the inset gives the single-parameter fit to the $n = 3$ data yielding , $m_{eff} = 5 \times 10^{-11}$ kg which is a factor of 660 lower than the mass of the $n = 1$ mode.

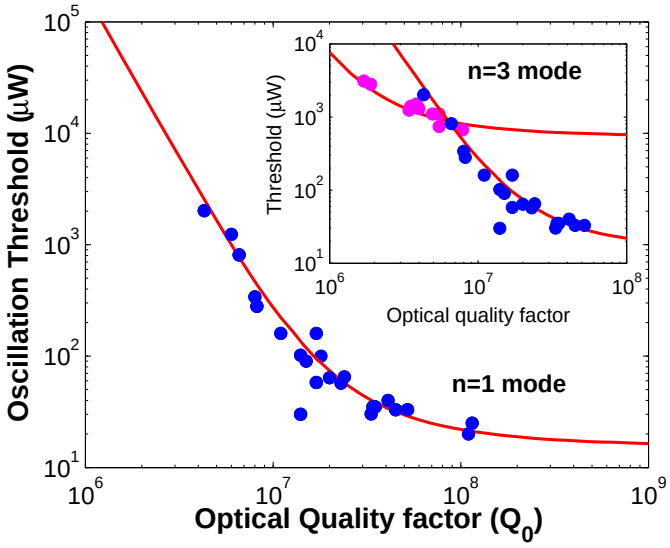

Fig. 15. Main panel shows the measured mechanical oscillation threshold (in micro-Watts) from Ref. [22] plotted versus the optical Q factor for the fundamental flexural mode ($n = 1$, $\Omega_m/2\pi = 4.4$ MHz, $m_{eff} \approx 3.3 \times 10^{-8}$ kg, $Q_m \approx 3500$). The solid line is a one-parameter theoretical fit obtained from the minimum threshold equation by first performing a minimization with respect to coupling (C) and pump wavelength detuning (Δ), and then fitting by adjustment of the effective mass. Inset: The measured threshold for the 3^{rd} order mode ($n = 3$, $\Omega_m/2\pi = 49$ MHz, $m_{eff} \approx 5 \times 10^{-11}$ kg, $Q_m \approx 2800$) plotted versus optical Q. The solid line gives again the theoretical prediction. The $n = 1$ data from the main panel is superimposed for comparison. Figure stems from reference [22].

4.3. Oscillation Linewidth

A further important characteristic of the regenerative mechanical oscillation is the linewidth of the mechanical oscillation frequency. Theoretically, the limit for the line-width in the case of temperatures $k_B T_R > \hbar\Omega_m$is set by classical, thermal noise and obeys the relationship [**?**,54,67]:

$$\Delta\Omega_m \cong \frac{k_B T_R}{P}\left(\frac{\Omega_m}{Q_m}\right)^2 \tag{24}$$

Here P is the power dissipated in the mechanical oscillator, i.e. $P = \Gamma_m m_{eff}\Omega_m^2 \langle x^2 \rangle$. Consequently the equation predicts that the line-width and mechanical amplitude satisfy $\Delta\Omega_m \propto 1/\langle x^2 \rangle$. Indeed, experimental work has confirmed this scaling in toroidal microcavities [67].The measured, inverse-quadratic dependence is presented in Figure 16. Fundamental linewidths that are sub Hertz have been measured, however, with improvements in mechanical Q

#88348 - $15.00 USD Received 8 Oct 2007; revised 7 Dec 2007; accepted 7 Dec 2007; published 10 Dec 2007

factor, these values are expected to improve, owing to the inverse-quadratic dependence appearing in the above formula.

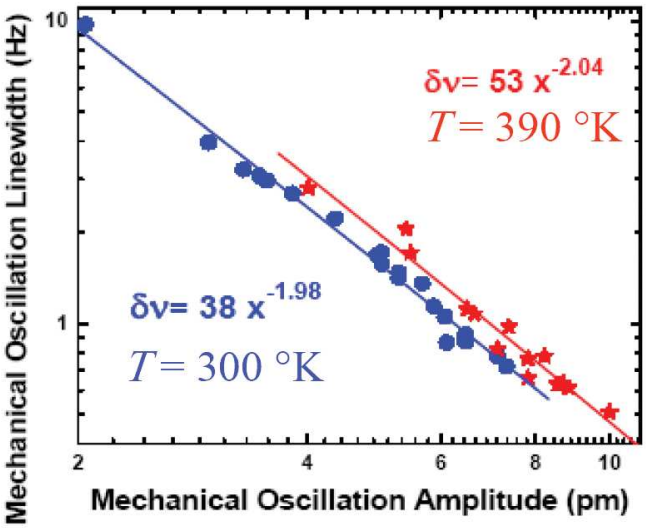

Fig. 16. Line-width measurements from Ref. [67] of the opto-mechanical oscillator for different amplitudes of oscillation plotted in picometers. The measurement is done at room temperature (dots) and at temperature 90 °C above room temperature (stars). The solid lines and the corresponding equations are the best fits to the log-log data. Solid line denotes theoretically expected behavior.

5. Red Detuning: Radiation Pressure Cooling

5.1. Experimental Setup

From the theoretical section it is clear that both cooling and amplification are indeed the same effect, albeit with opposite signs in the work performed on the mechanical system. Cooling was first theoretically noted by Braginksy [25], who proposed that red detuning could be used to "tranquilize" the mechanical modes of an interferometer. It has subsequently been considered in other work [22, 68]. While the manifestations of parametric amplification are readily observed (leading to a strong periodic modulation of the cavity transmission), the effect of cooling is more subtle as it decreases the Brownian motion of the mechanical motion. Consequently, the observation of cooling requires both a careful calibration of the mechanical displacement spectra and sufficient signal-to-noise to detect the *cooled* mechanical mode. Indeed, cooling was observed only after the parametric oscillation in a series of three experiments reported at the end of 2006, which employed coated micro-mirrors (in the Paris [26] and the Vienna [27] experiments) and toroidal micro-cavities [28] (at the MPQ in Garching). As mentioned earlier, there is no threshold condition for cooling (as in the case of the parametric oscillation), however, to achieve efficient temperature reduction the power injected when red detuning, must greatly exceed the threshold of the parametric oscillation instability for blue detuning.

Cooling in toroidal microcavities was observed by pumping with an external diode laser that is red detuned with respect to the optical resonance. It deserves notice that this detuning is intrinsically unstable owing to the thermal bi-stability effect [69] . The cavity absorption induced heating causes a change of the cavity path length, which subsequently causes a red-shift

#88348 - $15.00 USD Received 8 Oct 2007; revised 7 Dec 2007; accepted 7 Dec 2007; published 10 Dec 2007

of the cavity resonance. This feature leads to thermal, self-locking on the blue-sideband used to observe parametric amplification and oscillation, but simultaneously destabilizes locking on the red sideband. This has necessitated the implementation of fast electronic feedback to the laser, in order to be able to observe cooling. As an error signal, either the detected transmission signal was used directly or a signal derived from this by a frequency modulation technique [70]. The error signal is pre-amplified with a low-noise amplifier (DC - 1 MHz), the two outputs of which are fed to two, custom-built proportional-integral controllers with bandwidths on the order of 1 kHz and 1 MHz. Both controllers allow us to apply an offset to the error signal input, enabling continuous variation of the control set-point and thus constant detuning from line center. Without further amplification, the output of the slower controller is applied to a piezoelectric element actuating the grating in the laser to tune the laser emission frequency. For the compensation of fast fluctuations, the output from the faster controller is applied to a field effect transistor parallel to the laser diode. The consequent temporary change of diode current leads to the desired laser frequency adjustment. Laser emission power is affected only on the order of 5% and, since the output of the fast controller is high-pass filtered (cut-off $\gg$ 10 Hz), it remains unmodified on average.

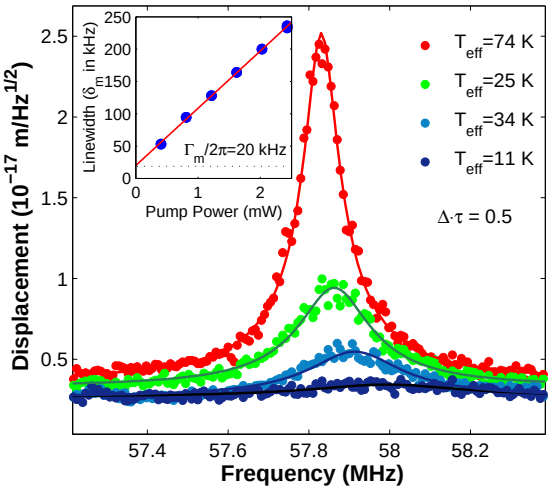

Fig. 17. Main figure shows the normalized, measured noise spectra around the mechanical breathing mode frequency for $\Delta \cdot \tau \approx -0.5$ and varying power ($0.25, 0.75, 1.25$,and 1.75 mW). The effective temperatures were inferred using mechanical damping, with the lowest attained temperature being 11K. (b) Inset shows increase in the linewidth (effective damping $\delta_m = \Gamma_{eff}/2\pi$) of the $57.8-$MHz mode as a function of launched power, exhibiting the expected linear behavior as theoretically predicted. From reference [28].

The described locking technique was used in Reference [28] to observe back-action cooling by radiation pressure. In the experiment the laser was detuned to $\Delta \cdot \tau \approx -0.5$. The mechanical mode under consideration in this study is a radial breathing mode with resonance frequency of 57.8 MHz. Since the mechanical mode is in thermal equilibrium with the environment at room temperature (T =300 K), it follows from the classical equipartition theorem that the mechanical oscillator undergoes Brownian motion.

#88348 - $15.00 USD Received 8 Oct 2007; revised 7 Dec 2007; accepted 7 Dec 2007; published 10 Dec 2007

5.2. *Experimental Observation of Cooling*

Given the high displacement sensitivity, it is possible to record important characteristics of the mechanical mirror motion, such as the resonance frequency $\Omega_m/2\pi$, damping rate and displacement spectral density $S_x(\omega)$. The determination of the intrinsic mechanical properties was carried out by injecting very-low power into the cavity, and recording the power spectral density with an electrical spectrum analyzer. Upon sufficiently low injected power, this leads to a nearly identical noise spectra for both blue and red detuning for $\Delta = \pm\kappa/2$ (since the mechanical amplification or cooling rate is much smaller than the intrinsic mechanical damping rate). Conversion to displacement spectral density then requires knowledge of the effective mass [52] of the mechanical mode which could be independently determined in two ways. First, from finite-element simulation of the actual cavity geometry parameters, as inferred from scanning electron microscopy images. As detailed in Ref [22] this is accomplished via the relation $m_{eff} = \frac{E_m}{\Omega_m^2(\delta R)^2}$, where δR is the mechanical displacement in the radial direction. Second, the effective mass was determined by experimental measurements, by recording the threshold for parametric oscillation for blue detuning and subsequently inverting the threshold equation for the effective mass. Note that in the described experiments, both techniques agree very well, from which the effective mass of the radial breathing mode of Figure 17 is inferred to be $m_{eff} = 1.5 \times 10^{-11}$kg . Correspondingly, the rms motion caused by Brownian motion of the radial breathing mode at room temperature is on the order of $\langle x^2 \rangle^{1/2} \approx 5 \times 10^{-14}$m.

Figure 17 shows the displacement spectral density for the radial breathing mode under conditions of constant red detuning ($\Delta = -\kappa/2$) for varying input power levels P. By extrapolating the resonant frequency and linewidth to zero power (cf. Inset) the intrinsic resonance frequency and an intrinsic mechanical Q factor of 2890 were extracted. Note that much higher mechanical Q $(> 50,000)$ are possible in an evacuated chamber [61] and by optimizing the micro-cavity shape to reduce dissipative clamping losses. In the reported experiment the optical line-width was 50 MHz, equivalent to an optical quality factor of 4.4×10^6. When varying the pump power, a clear reduction of the noise spectra is observed as shown in the main panel. The shape of the spectra changes in two dramatic ways. First the line-width of the mechanical spectra increase, owing to the fact that the light field provides a viscous force, thereby increasing the damping rate. Note that this rate varies linearly with applied power (cf. inset). Moreover, and importantly, the areas of the mechanical curves also reduce, which are a direct measure of the mechanical breathing modes (RBM) temperature. Indeed the effective temperature of the RBM is given by $k_B T_{eff} = \int \Omega^2 m_{eff} S_x(\Omega) d\Omega$ and correspondingly the peak of the displacement spectral density is reduced in a quadratic fashion with applied laser power. While measurement of the calibrated noise spectra is the most accurate way to determine the effective temperature, the simplified analysis presented earlier (and neglecting any other heating mechanism) yields a temperature (cf. Equation 19) given by the ratio of damping rates (with and without the pump laser):

$$T_{eff} \cong \frac{\Gamma_m}{\Gamma_m + \Gamma} T_R \tag{25}$$

As noted before this formula only proves valid when $\frac{\Gamma_m}{\Gamma_m+\Gamma} < 1/Q_m$ and for cooling rates satisfying $\Gamma << \kappa$. Note that the maximum temperature reduction factor is bound by the cavity decay rate $\tilde{\Gamma}/\kappa$. Thus, the highest temperature reduction factor which can be attained is given by $\sim \kappa/\Gamma_m$. Furthermore, additional modifications of this expression are necessary when entering the limit of temperatures, which correspond to only a few quanta, and will be considered in the next section.

For the highest pump power (2 mW and 970 nm), the effective temperature was reduced from 300 K to 11 K. This experiment, reported in Ref. [28], along with two earlier publica-

#88348 - $15.00 USD Received 8 Oct 2007; revised 7 Dec 2007; accepted 7 Dec 2007; published 10 Dec 2007

tions [26, 27] represent the first demonstration of radiation-pressure back-action cooling. It is noted for completeness that the experiment described in Ref [27] also attributed an appreciable cooling effect due to thermal effects in the mirror coatings. Indeed, of the physical mechanisms that can create opto-mechanical coupling temperature is another possibility. Temperature variations introduced by absorption, for example, create a well-known, trivial coupling, by way of thermal expansion. Indeed both mechanical amplification [71] and cooling [68] have been demonstrated using this mechanism. In the present, microtoroid studies, thermal effects are negligible. This is known, first, because of the parametric-instability studies of the previous section, where both the observed threshold dependence on optical Q as well as the magnitude of the threshold power, itself, are in excellent agreement with the theory of radiation-pressure-induced coupling. Second, the recent observation of microwave-rate parametric oscillations [63] confirms the broad-band nature of the underlying mechanism, greatly exceeding bandwidths possible by thermal coupling mechanisms.

To *quantitatively* assess the contributions of thermal and radiation-pressure induced effects in the present context, pump-probe-type response measurements were performed using a second laser coupled to the cavity and operating in the wavelength region around 1550 nm. This laser serves as *pump*, providing a sinusoidally modulated input power $P(t) = P_0(1+\varepsilon\sin(\Omega t))$, which in turn causes the optical resonances to periodically shift via both thermal effects and radiation-pressure-induced mechanical displacement, but also via the Kerr-nonlinearity of fused silica. These shifts are then "read out" with the 965 nm probe laser tuned to the wing of an optical resonance. Modulating the power of the pump laser and demodulating the detected probe power with the same frequency, it is possible to measure the micro-cavity response caused by all three nonlinearities (thermal, Kerr, and radiation pressure). Note that due to their different spectral response, the three nonlinearities can be readily differentiated when performing a frequency sweep. While electronic modulation and demodulation are conveniently accomplished with an electronic network analyzer, we use a fibre-coupled interferometric $LiNbO_3$ amplitude modulator to generate the modulated pump light. Data were taken on a logarithmic frequency scale between 50 Hz and 200 MHz, and, subsequently, on a linear frequency scale in the interval $50-65$ MHz. From finite-element simulation, this resonance can be identified as the radial breathing mode. The result of this measurement, as first reported in reference [28], is shown in figure 18. Several features are evident from the graph and are now discussed in detail.

First, the plateau in the response, for frequencies beyond 1 MHz and up to the cavity (and detector) cut-off at 200 MHz, is attributed to the intensity-dependent refractive index (Kerr effect) of fused silica [72, 73]. Importantly, since both thermal and mechanical responses exceed the Kerr non-linearity in some frequency domains, the Kerr effect (plateau) provides a precisely known reference for all observed nonlinearities. Second, the response up to a frequency of about 1MHz can be well fitted assuming the sum of two single-poled functions with cut-off frequencies of 1.6 kHz and 119 kHz. It has been attributed to the response related to convective and conductive heat exchange of the cavity mode with its environment [28, 58]. Concerning this thermal-related response function, it is important to note that a temperature change to the silica microcavity causes resonant frequency shifts via both a change in the refractive index and a displacement due to thermo-mechanical expansion. However, temperature-induced index changes dominate over thermal expansion by a factor of at least 15 for glass. Therefore, the thermo-mechanical contribution to the low-frequency-response shown in Figure 18 is, at least, one order-of-magnitude smaller than the total thermal response.

Finally, at 58 MHz in the response spectrum, the radiation-pressure-driven mechanical response is observable, which (inset Fig. 22) is a factor of $\times 260$ stronger than the Kerr nonlinearity in the present device. It is emphasized that this ratio is in quantitative agreement with the theoretically predicted Kerr-to-radiation pressure ratio. From the well-identified frequency

#88348 - $15.00 USD Received 8 Oct 2007; revised 7 Dec 2007; accepted 7 Dec 2007; published 10 Dec 2007

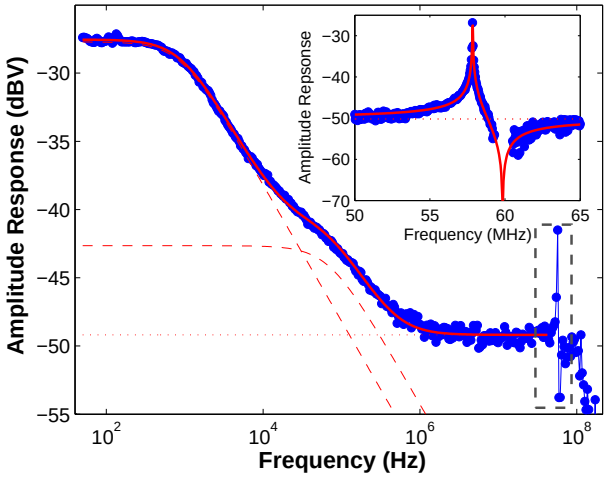

Fig. 18. The frequency response from $0-200\,\mathrm{MHz}$ of a toroidal opto-mechanical system, adopted from Reference [28]. The plateau occurring above $1\,\mathrm{MHz}$ is ascribed to the (instantaneous) Kerr nonlinearity of silica (dotted line). The high-frequency cutoff is due to both detector and cavity bandwidth. The response poles at low frequency are thermal in nature. Inset: Data in the vicinity of mechanical oscillator response shows the interference of the Kerr nonlinearity and the radiation pressure-driven micromechanical resonator (which, on resonance, is $\pi/2$ out-of phase with the modulating pump and the instantaneous Kerr nonlinearity). From the fits (solid lines) it can be inferred that the radiation pressure response is a factor of 260 larger than the Kerr response and a factor of $\times 100$ larger than the thermo-mechanical contribution.

response of the aforementioned thermal effects it is possible to conclude that the thermal effect contribution to the interaction of the cavity field with the $58\,\mathrm{MHz}$ radial breathing mode is at least 2 orders of magnitude too weak to explain the observed effects. Consequently, the response measurements give unambiguous proof that such thermal effects contribute less than 1 part in 100 to the observed cooling (or amplification) rate.

At a basic level, it is of significant importance that *optical forces* are dominant. These forces are both conservative and broadband, allowing for a Hamiltonian formulation [50], features that are fundamental to cavity-QOM physics as well as to potential applications of cavity-OM as a technology.

5.3. Quantum limits of radiation pressure back-action cooling

An important question is what limiting temperature is achievable with the radiation pressure back-action cooling technique as described above. Indeed, ground state cooling of harmonically bound ions and atoms has first been demonstrated by Wineland [74] almost two decades ago and has led to a remarkable set of advances in Atomic Physics, such as the generation of non-classical states of ion motion [75] or Schrödinger cat states [76]. Note that ground state cooling of mechanical oscillators is particularly challenging as the temperature corresponding to a single phonon corresponds to 50 μK for a 1 MHz oscillator, or 50 mK for a 1 GHz oscillator, which are only accessible by dilution refridgerators. Radiation-pressure back-action cooling might provide a route to achieve yet lower temperatures.

However, even the early work of Braginsky did not address the fundamental question of whether ground-state cooling is possible using the described mechanisms. Recently, two the-

#88348 - $15.00 USD Received 8 Oct 2007; revised 7 Dec 2007; accepted 7 Dec 2007; published 10 Dec 2007

oretical papers [48, 49] have extended the classical theory of radiation-pressure back-action cooling to the quantum regime and shown the close relationship that cavity back-action cooling has with the laser cooling of harmonically bound atoms and ions. While a detailed description of the theoretical framework can be found in references [48, 49] we here briefly recapitulate the main results in terms of the fundamental temperature limit.

In the quantum mechanical treatment, the mechanical oscillator is described in terms of its average occupancy n, where $n = 0$ designates the quantum ground state (in which the harmonic oscillator energy only contains the zero-point energy contribution). In brief and as shown in Refs [48,49], the quantum mechanical cooling limit is due to the fact that cooling proceeds both by motional increasing and decreasing processes. Motional decreasing (increasing) processes occur with a rate $R^{BSB} \propto \eta^2 A^- n$ ($R^{RSB} \propto \eta^2 A^+ (n+1)$), where n is the phonon occupancy, $A^{\pm} \propto \frac{1}{4(\Delta \mp \Omega_m)^2 + \kappa^2}$ are the lorentzian weights of the Stokes and anti-Stokes sidebands and $\eta = \frac{\omega_0 x_0}{\Omega_m R}$ an effective parameter [49] with $x_0 = \sqrt{\frac{\hbar}{m_{eff}\Omega_m}}$ being the zero point motion of the mechanical oscillator mode. Detailed balance [77] of the motional increasing and decreasing processes then yields the minimum final occupancy (neglecting reservoir heating):

$$n_f = \frac{A^+}{A^- - A^+} \tag{26}$$

In the unresolved $\kappa \gg \Omega_m$ side-band case, (which has been referred to as "weak binding" in Atomic Laser cooling [78]) this prevents ground state cooling as:

$$n_f \approx \frac{\kappa}{4\Omega_m} \gg 1 \tag{27}$$

Converting this expression into an equivalent temperature $T_D \approx \frac{\hbar\kappa}{4k_B}$, yields the *Doppler temperature* (as known in Atomic Laser Cooling). On the other hand, occupancies well below unity can be attained in the resolved sideband case $\Omega_m \gg \kappa$ yielding:

$$n_f \approx \frac{\kappa^2}{16\Omega_m^2} \ll 1 \tag{28}$$

If also the contribution from reservoir heating is included, the final occupancy that can be achieved then takes the form

$$n_f = \frac{A^+}{A^- - A^+} + \frac{\Gamma_m}{\Gamma_m + \Gamma} n_R \tag{29}$$

Here the n_R average denotes the average occupancy of the harmonic oscillator prior to applying radiation pressure cooling. As before, this limit is valid over the range where the cooling satisfies $\frac{\Gamma_m + \Gamma}{\Gamma_m} < n_R$ and $\Gamma < \kappa$. Note that from the above expression it becomes clear that precooling of the mechanical oscillators is advantageous and is indeed presently undertaken by several groups [30]. Resolved sideband cooling has also recently been demonstrated experimentally [47].

5.4. Physical Interpretation of the Quantum limits of Back-action Cooling

We next give some physical intuition into the above limits. It is worth noting that the above introduced temperature limits are in fact a direct manifestation of the *Heisenberg uncertainty principle* and are of rather general validity. This can be understood as follows. As shown in Section 2 the mechanical motion produces blue-shifted sidebands which remove mechanical quanta from the mechanical oscillator. These generated photons decay during the cavity lifetime

#88348 - $15.00 USD Received 8 Oct 2007; revised 7 Dec 2007; accepted 7 Dec 2007; published 10 Dec 2007

$1/\kappa$ into the outside world (i.e. into the tapered optical fiber waveguide, or through the finite reflection of the mirror in the case of a Fabry-Perot). The finite decay time of the cavity however entails that the energy that is carried away by a blue-shifted photon has a Heisenberg limited uncertainty of $\Delta E = \hbar/\Delta t \approx \hbar\kappa$. Consequently, the mean energy of the mechanical oscillator $E = \hbar\Omega_m(n+\frac{1}{2})$ cannot be lower than this limit, implying a final Doppler temperature of $T_D \approx \hbar\kappa/k_B$ in entire analogy to Laser Cooling in Atomic Physics [6]. This Doppler temperature entails that the final occupancy is much larger than unity in the case where the mechanical oscillator frequency is smaller than the cavity line-width (since $\kappa \gg \Omega_m$). In contrast, ground state cooling is possible when then energy quantum of the mechanical oscillator ($\hbar\Omega_m$) is made large in comparison with the energy scale set by the Doppler temperature. This required the "strong binding condition" to be satisfied, i.e. $\Omega_m \gg \kappa$.

A second consideration that can be used to successfully estimate the quantum limits of back-action cooling is to consider the mechanical mirror as performing a measurement on the intra-cavity photons. As in the case of photo-detector shot noise, the random arrival time of photons onto the mirror will entail a fluctuation of the radiation pressure force that will heat the mechanical oscillator. If N is the average number of photons in the cavity, the fluctuation of photon numbers (governed by Poissonian statistics) is given by $\sqrt{N}$, entailing a radiation pressure force fluctuation of $\left\langle \Delta F_{RP}^2 \right\rangle^{1/2} = \sqrt{N}\frac{2\hbar\kappa}{T_{rt}}$. Approximating this fluctuation as a white noise spectrum over the cavity bandwidth, the corresponding force spectral density of the radiation pressure quantum noise is given by $\delta F_{RP}^2(\Omega) = \left\langle \Delta F_{RP}^2 \right\rangle / \kappa$. This effectively white spectrum provides a driving force for the mechanical oscillator, and can be used to determine the final temperature via the relation $k_B T_f = \int \Omega^2 m_{eff} \left|\chi_{eff}(\Omega)\delta F_{RP}(\Omega)\right|^2 d\Omega = \Gamma^{-1} m_{eff} \left|\delta F_{RP}(\Omega_m)\right|^2$ (where $\chi_{eff}(\Omega)$ is the modified mechanical oscillators susceptibility). Two limits can be derived. First, assuming that the cavity line-width exceeds the mechanical oscillator frequency, the noise spectrum is approximately given by $\delta F_{RP}^2(\Omega) \approx \frac{P}{\hbar\omega}\frac{1}{2}\tau(\frac{\hbar k}{T_{rt}})^2 = \frac{P\hbar\omega}{2L^2}\tau^2$ which yields i.e. $k_B T_f \approx \hbar\kappa/4$ (i.e. $n_f \approx \frac{\kappa}{4\Omega_m}$ recovering the result derived in [48, 49]). Here we have assumed a Fabry Perot cavity of length L. On the other hand considering the resolved sideband regime (i.e. assuming laser and $\Delta = -\Omega_m$) the spectral density of the radiation pressure quantum fluctuations at the frequency of the mechanical oscillator are given $\delta F_{RP}^2(\Omega_m) \approx \frac{P\hbar\omega}{2L^2\Omega_m}$ by yielding the result $k_B T_f = \frac{\hbar\Omega_m}{2}(1+\frac{\kappa^2}{8\Omega_m^2})$ or $n_f \approx \frac{\kappa^2}{16\Omega_m^2}$. Thus, the final occupancy in the unresolved and resolved sideband case can be understood as arising from the quantum fluctuation of the intra-cavity field and are in agreement with the results of a rigorous calculation.

6. Summary and Outlook

In summary, we have described dynamical effects of radiation pressure in Cavity Opto-Mechanics. Specifically, both amplification and cooling of mechanical eigenmodes have been described as manifestations of finite-cavity-delay on mechanical oscillator's dynamics. Beyond the described phenomena of dynamical back-action, the Physics that can be studied in the field of Cavity Optomechanics encompasses several other areas of investigation. For instance, the classical dynamics of cavity Opto-mechanical systems exhibits a wide range of phenomena, ranging from dynamical multistability [53], static bistability [19] to chaotic regimes [62], some of which have already been observed in an experimental setting and allow one to create switchable tunable optical filters [44]. Furthermore, parametric amplification [22–24] of mechanical modes constitutes an entirely new way of creating the analogue of a 'photonic quartz oscillator" which is driven purely by the radiation pressure of light and whose line-width is limited by thermal noise. With continued improvements in mechanical Q that are already underway to address the requirements of cooling-related-research, there is the potential for realization of a new class of ultra-stable, narrow linewidth rf oscillators.

#88348 - $15.00 USD Received 8 Oct 2007; revised 7 Dec 2007; accepted 7 Dec 2007; published 10 Dec 2007

On the cooling side, there is a rich history of theoretical proposals pertaining to entangling mechanical oscillators with a light field using radiation pressure [12, 37, 38]. Most of these will require achieving temperatures at which the mechanical system is close-to, or at, the quantum ground state. With the rapid progress towards realization of ground-state cooling, it now seems likely that many of these ideas and proposals can be tested over the next decade. Similarly, macroscopic mechanical modes can provide a new medium in which to explore quantum information phenomena, as has been true in the rich scientific arena of cavity QED [79]. Indeed, one can view cavity QOM as the logical extension of cavity QED into the macroscopic realm.

Another interesting goal is to reach a regime where cavity QOM phenomena become observable. For example, a regime where the back-action from the quantum noise of the radiation pressure dominates the thermal noise [8, 9] would enable experimental realizations of proposals such as the quantum non-demolition measurement of photon number or pondermotive squeezing [12]. Moreover, recent work from Yale [30] has demonstrated Cavity OM systems which realize a quadratic coupling to the mechanical coordinate, thereby lending themselves to perform QND measurements of the mechanical eigenstate.

As originally noted, both cooling [25] ("tranquilizer") and parametric instability [80] were first conceived theoretically in the context of gravitational-wave detection by Braginsky. No doubt, the better understanding of these phenomena gained by their demonstration in the microscale will benefit this important field. Along these lines, since the initial observation of radiation pressure parametric instability in microtoroids [22–24] in 2005, the MIT gravitational-wave group has reported observation of parametric instability [81]. Even more recently they have also reported the cooling of gram scale mirror modes [29]. These results bode well for further progress in this field.

From a practical point-of-view, the ability to achieve cooling and oscillation of micromechanical modes on a semiconductor chip is important for realization of new technologies that could leverage these new tools. Specifically, miniaturization and integration of these functions with electronics and other optical functions is already possible because of this microfabricated, chip-based platform. Also significant is that radiation-pressure cooling through dynamic back action, as already noted, is a highly targeted form of cooling in which a selected mechanical mode(s) can be precisely defined to receive the benefit of cooling, while other modes remain at elevated or even at room temperature. Indeed, the first demonstrations of backaction cooling were to temperatures in the range of 10 K, but featured mechanical structures that were otherwise uncooled and at room temperature. As a result, this novel form of cooling offers ultra-low temperature performance with relatively low power requirements (milli-Watts) and without the need for cryogenics, vacuum handling, or any of the other necessities of conventional refrigeration. This feature, above all others, would seem to offer the greatest advantages in terms of new technologies.

Finally, the range of phenomena that have been described here extend over the entire electromagnetic spectrum. Indeed, the concept of dynamic back action was conceived-of first in the microwave realm [10]. It is also important to note that there are electro-mechanical systems that provide an analogous form of back action cooling [16, 18]. These systems can potentially provide a means to achieve the quantum ground-state.

In summary Cavity (Quantum) Opto-Mechanics represents many of the concepts of atomic and molecular physics, however embodied in an entirely different macroscale system. It is currently experiencing rapid experimental and theoretical success in various laboratories worldwide and offers entire new inroads for basic science and potentially new technologies. It seems clear that this field is entering an exciting period of experimental science.

#88348 - $15.00 USD Received 8 Oct 2007; revised 7 Dec 2007; accepted 7 Dec 2007; published 10 Dec 2007

Acknowledgements

KJV acknowledges the Caltech Lee Center and DARPA for supporting this work. TJK acknowledges support via a Max Planck Independent Junior Research Group, a Marie Curie Excellence Grant (MEXT-CT-2006-042842), a Marie Curie Reintegration Grant and the Nanosystems Initiative Munich (NIM). The authors kindly thank Albert Schliesser, Olivier Arcizet, Jens Dobrindt and Mani Hossein-Zadeh for contributions to this review.

#88348 - $15.00 USD Received 8 Oct 2007; revised 7 Dec 2007; accepted 7 Dec 2007; published 10 Dec 2007